

Reversible Displacement of Polyagostic Interactions in 16e $[\text{Mn}(\text{CO})(\text{R}_2\text{PC}_2\text{H}_4\text{PR}_2)_2]^+$ by H_2 , N_2 , and SO_2 . Binding and Activation of $\eta^2\text{-H}_2$ trans to CO Is Nearly Invariant to Changes in Charge and cis Ligands

Wayne A. King, Brian L. Scott, Juergen Eckert, and Gregory J. Kubas*

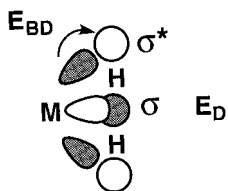
Los Alamos National Laboratory, CST-18, MS-J514, Los Alamos, New Mexico 87545

Received October 29, 1998

Electrophilic 16e $[\text{Mn}(\text{CO})(\text{R}_2\text{PC}_2\text{H}_4\text{PR}_2)_2]^+$ complexes ($\text{R} = \text{Et}, \text{Ph}$) are synthesized by metathesis of $\text{MnBr}(\text{CO})(\text{R}_2\text{PC}_2\text{H}_4\text{PR}_2)_2$ with Na or Li salts of low-coordinating boron or gallium anions (e.g., $[\text{B}\{\text{C}_6\text{H}_3(3,5\text{-CF}_3)_2\}_4]^-$ or $[\text{Ga}(\text{C}_6\text{F}_5)_4]^-$). They contain weak polyagostic interactions that are reversibly displaced by H_2 , N_2 , and SO_2 (which is a surprisingly weak ligand here). The agostic and H_2 complexes, as well as the gallium anions including the new species $[\{\text{Ga}(\text{C}_6\text{F}_5)_3\}(\mu\text{-Cl})]^-$, have been characterized by NMR, IR, and X-ray crystallography. The agostic Mn–H distances (e.g., 2.9 Å) are much longer than those found for the single agostic interactions in $\text{Mo}(\text{CO})(\text{diphosphine})_2$ and $[\text{Mn}(\text{CO})_3(\text{PCy}_3)_2]^+$. The H–H and also the Mn–H distances have been determined in the H_2 complex by T_1 measurements for both the H_2 and HD isotopomers. IR data and C–O and M–C bond lengths are used to gauge the π -acceptor strengths of ligands trans to the CO. The agostic C–H bonds are the weakest ligands and also the weakest acceptors, but the H_2 ligand is an excellent acceptor as strong as N_2 and ethylene. The variation of $\nu(\text{CO})$ on increasing the basicity of the cis-phosphine (dppe versus depe) in $\text{trans-M}(\text{CO})(\text{diphosphine})_2(\text{L})$ is less than expected and far less than that on increasing the charge on the complex ($\text{M} = \text{Mn}^+$ versus Mo). The H–H bond lengths (0.87–0.90 Å) and $J(\text{HD})$ NMR couplings (32–34 Hz) in $[\text{Mn}(\text{CO})(\text{R}_2\text{PC}_2\text{H}_4\text{PR}_2)_2(\text{H}_2)]^+$ and other cationic H_2 complexes with trans-CO are strikingly similar to their neutral analogues and nearly invariant. Activation of H–H in the more electrophilic cationic systems occurs primarily via increased σ donation from H_2 as compared to the more electron-rich neutral analogues where back-bonding dominates. The nature of the ligand trans to H_2 (the strong acceptor CO here) controls the H–H distance more so than all of the cis ligands combined, especially for cationic complexes.

Introduction

The activation of H–H and other strong, inert σ bonds on transition-metal centers is a foundation of catalysis and many types of chemical/biochemical conversions. Metal– H_2 binding and by analogy X–H coordination are governed by both σ donation from the X–H bond to the metal (E_D) and π back-bonding from metal to X–H σ^* (E_{BD}). The relative strength of



each bonding component has been quantified computationally by both Ziegler¹ and Frenking² and is dependent on the electronic nature of the ancillary ligands. Donor ligands enhance E_{BD} while acceptors promote increased E_D , and there is a fine balance between the effects. For example, the M– H_2 bonding energy in electron-poor $\text{Mo}(\text{CO})_5(\text{H}_2)$ has a high E_D and much smaller

E_{BD} but is closer than expected to that in $\text{Mo}(\text{CO})(\text{R}_2\text{PC}_2\text{H}_4\text{PR}_2)_2(\text{H}_2)$, where E_{BD} is high and E_D is lower.^{1b} Dihydrogen is an extremely versatile ligand and can bind to highly electrophilic systems because of this amphoteric behavior. Importantly, excessive back-bonding promotes X–H rupture, i.e., oxidative addition (OA) but increasing σ donation from the X–H bond to the metal cannot by itself give OA. We have recently focused on developing highly electrophilic cationic fragments³ such as $[\text{Mn}(\text{CO})(\text{dppe})_2]^+$, $[\text{Mn}(\text{CO})_3(\text{PCy}_3)_2]^+$, $[\text{PtH}(\text{PPri}_3)_2]^+$, and $[\text{Re}(\text{CO})_4(\text{PCy}_3)]^+$ for systematic studies of the binding of H_2 , silanes, and potentially, alkanes (dppe = $\text{Ph}_2\text{PC}_2\text{H}_4\text{PPh}_2$). The positive charge here favors η^2 coordination over OA, and the degree of activation of the H–H bond in these and other cationic or dicationic H_2 complexes is remarkably similar to that in neutral analogues, as judged by H–H distance, $J(\text{HD})$, and other parameters. For example, despite their increasing charge and electrophilicity, the isoelectronic 16e fragments $\text{Mo}(\text{CO})(\text{dppe})_2$,⁴ $[\text{Mn}(\text{CO})(\text{dppe})_2]^+$,^{3a} and $[\text{M}(\text{CO})(\text{diphosphine})_2]^{2+}$ (M

- (1) (a) Li, J.; Dickson, R. M.; Ziegler, T. *J. Am. Chem. Soc.* **1995**, *117*, 11482. (b) Li, J.; Ziegler, T. *Organometallics* **1996**, *15*, 3844.
 (2) (a) Dapprich, S.; Frenking, G. *Angew. Chem., Int. Ed. Engl.* **1995**, *34*, 354. (b) Ehlers, A. W.; Dapprich, S.; Vyboishchikov, S. F.; Frenking, G. *Organometallics* **1996**, *15*, 105. (c) Frenking, G.; Pidum, U. *J. Chem. Soc., Dalton Trans.* **1997**, 1653. (d) Dapprich, S.; Frenking, G. *Organometallics* **1996**, *15*, 4547.

- (3) (a) King, W. A.; Luo, X.-L.; Scott, B. L.; Kubas, G. J.; Zilm, K. W. *J. Am. Chem. Soc.* **1996**, *118*, 6782. (b) Butts, M. D.; Kubas, G. J.; Scott, B. L. *J. Am. Chem. Soc.* **1996**, *118*, 11831. (c) Huhmann-Vincent, J.; Scott, B. L.; Kubas, G. J. *J. Am. Chem. Soc.* **1998**, *120*, in press. (d) Toupadakis, A. I.; Kubas, G. J.; King, W. A.; Scott, B. L.; Huhmann-Vincent, J. *Organometallics*, submitted for publication. (e) Hay, P. J.; Kubas, G. J., manuscript in preparation.
 (4) (a) Kubas, G. J.; Burns, C. J.; Eckert, J.; Johnson, S.; Larson, A. C.; Vergamini, P. J.; Unkefer, C. J.; Khalsa, G. R. K.; Jackson, S. A.; Eisenstein, O. *J. Am. Chem. Soc.* **1993**, *115*, 569. (b) Sato, M.; Tatsumi, T.; Kodama, T.; Hidai, M.; Uchida, T.; Uchida, Y. *J. Am. Chem. Soc.* **1978**, *100*, 447.

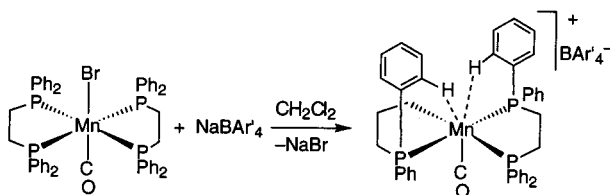
Table 1. Infrared and NMR Data

complex	$\nu(\text{CO})^a$	$\delta \text{ } ^1\text{H}^b$	$\delta \text{ } ^{31}\text{P}\{\text{ } ^1\text{H}\}$
MnBr(CO)(depe) ₂	1803	2.30, 1.86, 1.69, 1.19	74.2
[Mn(CO)(depe) ₂][BAR' ₄]	1853	1.59, 1.39, 0.92	81.4
[Mn(CO)(depe) ₂][Ga(C ₆ F ₅) ₄]		1.8–0.7	80.3
[Mn(CO) ₂ (depe) ₂][BAR' ₄]	1888	1.90, 1.66, 1.24	75.8
[Mn(CO)(depe) ₂ (H ₂)][BAR' ₄]	1887	1.65, 1.22, 0.93, 0.71, –10.25	83.5
[Mn(CO)(depe) ₂ (H ₂)][Ga(C ₆ F ₅) ₄]		1.7–0.8, –10.23	83.4
[Mn(CO)(depe) ₂ (D ₂)][Ga(C ₆ F ₅) ₄]		1.5–0.6	83.3
[Mn(CO)(depe) ₂ (N ₂)][BAR' ₄]	1896	1.68, 1.53, 1.39, 0.94	72.6
MnBr(CO)(dppe) ₂	1821		
[Mn(CO)(dppe) ₂][BAR' ₄]	1862 [1839]	7.3–7.0, 6.16, 2.79	82.6
[Mn(CO)(dppe) ₂][Ga(C ₆ F ₅) ₄]		7.3–7.0, 6.23, 2.79	83.0
[Mn(CO)(dppe) ₂ (H ₂)][BAR' ₄]	[1896]	7.4–7.0, 2.52, 2.24, –7.23	85.5
[Mn(CO)(dppe) ₂ (H ₂)][Ga(C ₆ F ₅) ₄]		7.4–7.0, 2.50, 2.24, –7.22	85.7
[Mn(CO)(dppe) ₂ (D ₂)][Ga(C ₆ F ₅) ₄]		7.4–7.0, 2.50, 2.24	85.9
[Mn(CO)(dppe) ₂ (N ₂)][BAR' ₄]	1911	7.3–7.1, 6.67, 2.67, 2.34	75.0

^a In cm⁻¹ for Nujol mulls except for values in brackets (for dichloromethane solution). ^b In ppm for fluorobenzene (depe complexes) or dichloromethane (dppe complexes) solutions. All are multiplets except the broad high-field singlet for the H₂ ligand. Anion resonances are not listed (see Experimental Section). The field strength was 300 MHz, except for data where the PC₂H₄P bridge multiplet was resolved into several multiplets (500 MHz).

= Fe, Ru, Os)⁵ all coordinate H₂ reversibly trans to CO, with H–H distances near 0.88 Å and $J(\text{HD}) = 32\text{--}34$ Hz. The recent phosphite analogues, [Mn(CO){P(OR)₃}]₄⁺, also display these properties.⁶ The presence of the strong π -acceptor CO trans to H₂ is a crucial factor in these systems and greatly moderates the lengthening of the H–H bond.

As reported in a preliminary communication,^{3a} the cationic 16e complex [Mn(CO)(R₂PC₂H₄PR₂)₂]⁺ where R = Ph was readily prepared by metathesis of MnBr(CO)(R₂PC₂H₄PR₂)₂ with salts of the low-coordinating anion B[C₆H₃(3,5-CF₃)₂]₄⁻ (BAR'₄⁻), which is necessary to stabilize these highly reactive cations. Herein we report in detail the complexes for both R =



Et and R = Ph and also the use of gallium-based anions as useful alternates to boron-based anions.¹⁰ B is an interference in neutron scattering studies of cationic H₂ complexes and other compounds, and development of non-boron-containing, low-interacting counterions is important for such studies. The unsaturated cations contain weak polyagostic C–H interactions trans to CO that are displaced by H₂, N₂, and SO₂, which is an abnormally weak ligand here. Surprisingly, increasing the donor ability of the phosphines by varying R from Ph to Et in [Mn(CO)(R₂PC₂H₄PR₂)₂(H₂)]⁺ has only a minor effect on the activation of H₂. This points to the important concept that *the influence of the cis-ligand set on H₂ activation can be inconsequential and is nearly always far less important than that of the trans ligand*. As will be shown, this seems to be particularly true for cationic systems where back-bonding is lower.

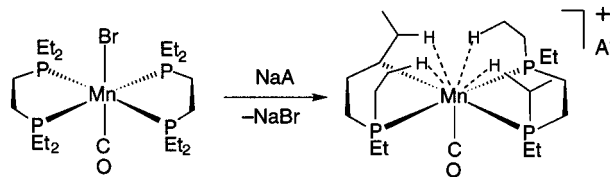
Results

Synthesis of MnBr(CO)(depe)₂. MnBr(CO)(depe)₂ is prepared as a yellow, moderately air-sensitive solid by photolysis

of MnBr(CO)₅ in benzene in the presence of excess depe in a procedure analogous to that previously reported for MnBr(CO)(dppe)₂.⁷ ¹H NMR displays a multiplet at δ 1.1–2.3 resolvable into four nonintegrable overlapping components (Table 1). The presence of four resonances is consistent with Br trans to CO and the depe ligands coordinated in a plane if it is assumed that the chemical shift differences of the Et groups above and below the plane are unresolved. ³¹P{¹H} NMR shows a single resonance at δ 74.2 also consistent with Br trans to CO. IR spectra reveal a strong CO band at 1803 cm⁻¹ comparable to that for MnBr(CO)(dppe)₂ (1821 cm⁻¹). The lowering of the CO stretch reflects increased π back-donation from Mn to CO on substitution of dppe by the better donor depe.

Synthesis of Li[Ga(C₆F₅)₄]. Li[Ga(C₆F₅)₄] is prepared by reaction of a slight excess of LiC₆F₅ with GaCl₃ in hexane at –78 °C. ¹H and ¹⁹F NMR spectra are consistent with those reported for [Bu₄N][Ga(C₆F₅)₄].⁸ Although elemental analysis of Li[Ga(C₆F₅)₄] yields inconsistent results owing to entrapment of solvent and unidentified fluorocarbon impurities observed by ¹⁹F NMR, the material can be used for subsequent reactions without further purification. Pure samples of Li[Ga(C₆F₅)₄] are prepared as the etherate Li[Ga(C₆F₅)₄]·2Et₂O by reaction of Ga(C₆F₅)₃·Et₂O^{8,9} with 1 equiv of LiC₆F₅ in Et₂O at –78 °C. Li[Ga(C₆F₅)₄]·2Et₂O was not used as starting material in the synthesis of [Mn(CO)(diphosphine)₂]⁺ because Et₂O can serve as a weak ligand.

Synthesis of [Mn(CO)(depe)₂][A] (A = BAR'₄, Ga(C₆F₅)₄). Stoichiometric reaction of NaBAR'₄ with MnBr(CO)(depe)₂ in fluorobenzene conveniently yields [Mn(CO)(depe)₂][BAR'₄]⁺ as a deep blue formally 16e complex analogous to the similarly prepared [Mn(CO)(dppe)₂][BAR'₄]⁺.^{3a} The bromide is metathe-



sized off the complex as NaBr, giving a cationic system with a

- (5) (a) Forde, C. E.; Landau, S. E.; Morris, R. H. *J. Chem. Soc., Dalton Trans.* **1997**, 1663. (b) Rocchini, E.; Mezzetti, A.; Rugger, H.; Burckhardt, U.; Gramlich, V.; Zotto, A. D.; Martinuzzi, P.; Rigo, P. *Inorg. Chem.* **1997**, *36*, 711.
 (6) Albertin, G.; Antoniutti, S.; Bettiol, M.; Bordignon, E.; Busatto, F. *Organometallics* **1997**, *16*, 4959.

- (7) Reimann, R. H.; Singleton, E. *J. Organomet. Chem.* **1972**, *38*, 113.
 (8) Ludovici, K.; Tyrra, W.; Naumann, D. *J. Organomet. Chem.* **1992**, *441*, 363.
 (9) Pohlmann, J. L. W.; Brinckmann, F. E. *Z. Naturforsch., Teil B*, **1965**, *20*, 5.

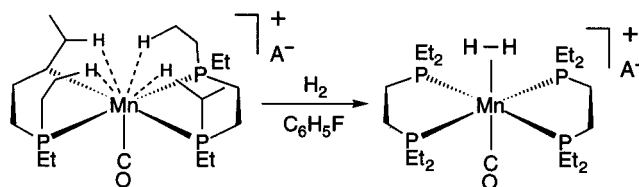
noncoordinating anion (A) and polyagostic interactions. Unlike the dppe congener, the depe complex is extremely sensitive to oxidation by air and CH_2Cl_2 and coordination by trace N_2 . In fact, the high sensitivity of this system to oxidation makes study by in situ generation in an NMR tube preferable to bulk synthesis. A preparative scale reaction under Ar gives crystalline $[\text{Mn}(\text{CO})(\text{depe})_2][\text{BAR}'_4]$ containing a small amount of $[\text{Mn}(\text{CO})_2(\text{depe})_2][\text{BAR}'_4]$ (identified by ^{31}P NMR) resulting from oxidation by trace dioxygen and transfer of released CO to $[\text{Mn}(\text{CO})(\text{depe})_2]^+$. The identity of $[\text{Mn}(\text{CO})_2(\text{depe})_2]^+$ is confirmed by reaction of in situ generated agostic complex with CO in an NMR tube reaction, as discussed below. Although isolated $[\text{Mn}(\text{CO})(\text{depe})_2]^+$ contains up to 15% dicarbonyl complex from integration of ^{31}P NMR spectra, a strong CO band is observable at 1853 cm^{-1} which is slightly lower than that for the more electrophilic dppe congener (1862 cm^{-1}). The higher $\nu(\text{CO})$ of the agostic cation as compared to the parent bromide complex is consistent with a more electron-deficient species. A CO band observed at 1889 cm^{-1} is assigned to the dicarbonyl impurity, as confirmed by independent synthesis (1888 cm^{-1}).

All detailed NMR studies of the agostic complex were performed on material generated in situ. ^1H NMR in $\text{C}_6\text{D}_5\text{F}$ revealed a multiplet at δ 0.9–1.6 from the depe ligand and two resonances at δ 8.32 and 7.65 typical for the BAR'_4 anion.^{3a,10} The multiplet was resolved in the 500 MHz spectrum (298 K) into three overlapping broad components at δ 1.59, 1.39, and 0.92. On cooling the sample to 228 K, the latter signals shifted to δ 1.72, 0.99, and 0.22 and gained fine structure, but no signals for the agostic interactions were observed. The resonances for the anion shifted to δ 8.50 and 7.55. $^{31}\text{P}\{^1\text{H}\}$ NMR in $\text{C}_6\text{D}_5\text{F}$ at 298 K yielded a singlet at δ 81.4 that shifted slightly to δ 83.5 on cooling to 228 K. This is consistent with a highly fluxional formally five-coordinate complex analogous to the dppe congener.^{3a} The existence of three major resonances in the ^1H NMR is also consistent with $[\text{Mn}(\text{CO})(\text{depe})_2]^+$ existing in solution as a fluxional species. Variable temperature studies in this system were limited by the relatively high freezing point of fluorobenzene ($-40\text{ }^\circ\text{C}$).

Addition of CO to a freshly generated sample of $[\text{Mn}(\text{CO})(\text{depe})_2]^+$ in fluorobenzene resulted in formation of a light yellow solution of $[\text{Mn}(\text{CO})_2(\text{depe})_2]^+$. ^1H NMR ($\text{C}_6\text{D}_6\text{F}$) revealed a multiplet at δ 1.9–1.2 that was resolved at 300 MHz into three overlapping multiplets for the depe ligand (Table 1). $^{31}\text{P}\{^1\text{H}\}$ NMR showed one resonance, and one CO stretch was identified in the IR, consistent with trans CO as in $[\text{Mn}(\text{CO})_2(\text{dppe})_2]\text{PF}_6$.¹¹

$[\text{Mn}(\text{CO})(\text{depe})_2][\text{Ga}(\text{C}_6\text{F}_5)_4]$ is generated in situ in an NMR tube by the reaction of excess $\text{Li}[\text{Ga}(\text{C}_6\text{F}_5)_4]$ (the amounts required vary according to purity) with $\text{MnBr}(\text{CO})(\text{depe})_2$. The properties and color of the $[\text{Ga}(\text{C}_6\text{F}_5)_4]^-$ salt are identical to those of the BAR'_4^- salt. Changing the anion has little effect on the NMR spectroscopy of the cation, although small shifts in the signals are seen (Table 1).

Synthesis of $[\text{Mn}(\text{CO})(\text{depe})_2(\text{H}_2)][\text{A}]$. The H_2 complex is cleanly generated by stoichiometric reaction of $\text{Na}[\text{BAR}'_4]$ with $\text{MnBr}(\text{CO})(\text{depe})_2$ in fluorobenzene under an atmosphere of H_2 . The resulting yellow solution readily loses H_2 in vacuo at room temperature, as evidenced by the appearance of the color of



the dark blue agostic complex, but not at $-78\text{ }^\circ\text{C}$ in frozen fluorobenzene. The H_2 complex is less oxygen sensitive than the agostic complex and is isolated by precipitation with hexane under H_2 or even He, where little dissociation is observed (although the light yellow microcrystalline complex will slowly lose H_2 , which is more rapid in vacuo). The depe complex loses H_2 much less readily than the dppe complex owing to the greater donor strength of depe and perhaps weaker agostic ethyl interactions.

^1H NMR for $[\text{Mn}(\text{CO})(\text{depe})_2(\text{H}_2)][\text{BAR}'_4]$ in $\text{C}_6\text{D}_5\text{F}$ displayed a multiplet at δ 1.7–0.7 for depe which was resolved at 500 MHz into four major overlapping multiplets. The broad H_2 resonance, integrating to two protons, was located at δ -10.25 (19 Hz fwhm, 500 MHz), which displayed no observable ^{31}P coupling. A comparison to the δ -7.23 resonance for the dppe analogue reveals greater shielding of H_2 in the depe system, again consistent with the greater donor properties of depe. The HD complex, prepared by reacting in situ generated agostic complex with HD gas, yielded a coupling constant of 33 Hz indicative of a short H–H distance. The value for the dppe analogue is only slightly less at 32 Hz. An estimated H–H distance of 0.87–0.89 Å for the depe complex was calculated from $J(\text{HD})$ using the correlations¹² of Morris and Heinekey and is similar to that for the dppe system as measured by solid-state NMR (0.89(2) Å).^{3a} Observation of a single ^{31}P resonance and four major ^1H resonances for the depe ligand is consistent with H_2 trans to CO. On cooling the sample from 298 to 228 K, ^1H NMR revealed small shifts for the depe ligands, the anion, and the H_2 ligand (to δ -10.33 , with significant broadening to 72 Hz (fwhm, 500 MHz)). No resonances associated with an oxidative addition product were observed. The $^{31}\text{P}\{^1\text{H}\}$ NMR signal at 228 K was unshifted, and no other resonances were observed. IR data showed a strong CO band at 1887 cm^{-1} , which is higher than that for the agostic complex and similar to that for $[\text{Mn}(\text{CO})_2(\text{depe})_2]^+$, indicating that the H_2 is removing electron density from the metal center through π back-bonding like a CO ligand.

$[\text{Mn}(\text{CO})(\text{depe})_2(\text{H}_2)][\text{Ga}(\text{C}_6\text{F}_5)_4]$ is prepared by the reaction of excess $\text{LiGa}(\text{C}_6\text{F}_5)_4$ with $\text{MnBr}(\text{CO})(\text{depe})_2$ under H_2 in fluorobenzene. The properties and NMR spectroscopy of the boron and gallium salts are for the most part identical. The D_2 complex is prepared under D_2 and yields NMR spectra similar to that for the H_2 species except for the absence of the signal for the H_2 ligand.

Synthesis of $[\text{Mn}(\text{CO})(\text{dppe})_2][\text{Ga}(\text{C}_6\text{F}_5)_4]$ and Its H_2 Adduct. Deep blue microcrystals of $[\text{Mn}(\text{CO})(\text{dppe})_2][\text{Ga}(\text{C}_6\text{F}_5)_4]$ are prepared by reaction of excess $\text{Li}[\text{Ga}(\text{C}_6\text{F}_5)_4]$ with $\text{MnBr}(\text{CO})(\text{dppe})_2$ under Ar in CH_2Cl_2 , using procedures identical to those for the preparation of the BAR'_4 salt.^{3a} ^1H NMR in CD_2Cl_2 revealed two multiplets at δ 7.3–7.0 and 6.23 for the Ph groups and a single multiplet at δ 2.79 for the bridging Et group of dppe. $^{31}\text{P}\{^1\text{H}\}$ NMR showed a singlet at δ 83.0. These results, particularly the single multiplet for the $\text{PC}_2\text{H}_4\text{P}$

(10) (a) Heinekey, D. M.; Schomber, B. M.; Radzewich, C. E. *J. Am. Chem. Soc.* **1994**, *116*, 4515. (b) Brookhart, M.; Grant, R. G.; Volpe, A. F., Jr. *Organometallics* **1992**, *11*, 3920. (c) Heinekey, D. M.; Radzewich, C. E.; Voges, M. H.; Schomber, B. M. *J. Am. Chem. Soc.* **1997**, *119*, 4172.

(11) Garcia-Alonso, F. J.; Riera, V. *Transition Met. Chem.* **1985**, *10*, 19.

(12) (a) Maltby, P. A.; Schlaf, M.; Steinbeck, M.; Lough, A. J.; Morris, R. H.; Klooster, W. T.; Koetzle, T. F.; Srivastava, R. C. *J. Am. Chem. Soc.* **1996**, *118*, 5396. (b) Luther, T. A.; Heinekey, D. M. *Inorg. Chem.* **1998**, *37*, 127.

bridge, are consistent with those found for the BAR'_4 salt (Table 1), indicating that the cation is fluxional in solution.^{3a}

The H_2 complex was prepared as above except under H_2 in CH_2Cl_2 using procedures similar to those for the preparation of the BAR'_4 salt.^{3a} $[\text{Mn}(\text{CO})(\text{dppe})_2(\text{H}_2)][\text{Ga}(\text{C}_6\text{F}_5)_4]$ can also be prepared by placing a CH_2Cl_2 solution of the agostic complex under H_2 and precipitating with hexane (direct reaction with H_2 in solid state fails). ^1H NMR showed a multiplet at δ 7.4–7.0 for the Ph groups and two multiplets at δ 2.50 and 2.24 for the Et bridge of dppe. The dihydrogen ^1H resonance was observed at δ -7.22 (33 Hz fwhm at 300 Hz). The NMR signals for the $[\text{Ga}(\text{C}_6\text{F}_5)_4]^-$ salt in CD_2Cl_2 are virtually identical to those for the BAR'_4 salt, indicating that the cation has an octahedral geometry with CO trans to H_2 and is unaffected by the anion.

The value of $T_1(\text{min})$ for the H_2 ligand in $[\text{Mn}(\text{CO})(\text{dppe})_2(\text{H}_2)][\text{Ga}(\text{C}_6\text{F}_5)_4]$ was determined to be 15.2(2) ms at 286 K at 300 K in CD_2Cl_2 and 116(8) ms for the HD analogue, which are valuable measurements, as will be shown here. H–H distances can be determined by T_1 measurements, although the effects of relaxation of the metal center on the H_2 ligand must be considered.¹³ Because ^{55}Mn possesses a nuclear spin of 5/2, the H–H distance measured in manganese– H_2 complexes will be systematically shortened by relaxation of the H_2 ligand caused by the metal center, R_{HMn} . This is in addition to the effects of relaxation caused by the ancillary ligands, $R_{\text{H-ligand}}$. This is expressed in eq 1 where $R = 1/T_1$.

$$R_{\text{HH}(\text{obs})} = R_{\text{HH}} + R_{\text{HMn}} + R_{\text{Hligand}} \quad (1)$$

The contribution to the relaxation of the hydrogen in the Mn–HD complex can be similarly expressed in eq 2.

$$R_{\text{HD}(\text{obs})} = R_{\text{HD}} + R_{\text{HMn}} + R_{\text{Hligand}} \quad (2)$$

Subtracting eq 2 from eq 1 will allow the effects of metal- and ligand-based relaxation on the dihydrogen ligand to be canceled out (eq 3).

$$R_{\text{HH}(\text{obs})} - R_{\text{HD}(\text{obs})} = R_{\text{HH}} - R_{\text{HD}} \quad (3)$$

Expressions for relating $1/T_1^{\text{min}}$ (HH) and $1/T_1^{\text{min}}$ (HD) values to H–H and H–D distances at 300 MHz field strength can be derived from the relationships in Desrosiers, et al.^{13b} A similar assumption that the rotational correlation coefficient T_c will be approximately the same for both metal– H_2 and –HD complexes is made.^{13b} A further assumption was made that the interatomic distances r_{HH} and r_{HD} in the H_2 and HD ligands are the same. The values for R_{HH} and R_{HD} are calculated from the expressions given in the Appendix and can be inserted into eq 3 to give eqs 4 and 5.

$$R_{\text{HH}(\text{obs})} - R_{\text{HD}(\text{obs})} = (1.29 \times 10^{-46})/r_{\text{HH}}^6 - (8.20 \times 10^{-48})/r_{\text{HD}}^6 \quad (4)$$

$$R_{\text{HH}(\text{obs})} - R_{\text{HD}(\text{obs})} = (1.21 \times 10^{-46})/r_{\text{HH}}^6 \quad (\text{assuming } r_{\text{HH}} \approx r_{\text{HD}}) \quad (5)$$

These relationships are derived for a nonrotating dihydrogen ligand. For a rapidly rotating dihydrogen ligand, the correction

to the spectral density function proposed by Morris must be used.^{13a} The constants in the above equations thus must be multiplied by 0.25. Finally, on substituting the observed relaxation values into eq 5 (R in units of s^{-1} and r_{HH} in cm), a value of 0.91(2) Å for the H–H distance is obtained that agrees well with that determined by solid-state NMR (0.89(2) Å).^{3a}

If the $R_{\text{H-ligand}}$ contributions are small, an equation for the distance from Mn to the hydrogen atoms in the H_2 ligand can be derived using similar expressions and assumptions.

$$R_{\text{HH}(\text{obs})} = R_{\text{HH}} + R_{\text{HMn}} \quad (6)$$

$$R_{\text{HH}(\text{obs})} = (1.29 \times 10^{-46})/r_{\text{HH}}^6 - (9.01 \times 10^{-47})/r_{\text{HMn}}^6 \quad (7)$$

On substitution of $r_{\text{HH}}^6 = (1.21 \times 10^{-46})/(R_{\text{HH}(\text{obs})} - R_{\text{HD}(\text{obs})})$ into eq 7, eq 8 can be derived.

$$1.07R_{\text{HD}(\text{obs})} - 0.07R_{\text{HH}(\text{obs})} = (9.01 \times 10^{-47})/r_{\text{HMn}}^6 \quad (8)$$

When the appropriate values are substituted into eq 8, a value of 1.64(3) Å is obtained for the Mn–H distance, which is reasonable when compared to the neutron diffraction value of 1.601(16) Å in $\text{MnH}(\text{CO})_5$.¹⁴ Often there is little variation in M–H distance in H_2 and hydride complexes. This general method is potentially useful to measure metal–dihydrogen coordination geometries in other related systems. It is noteworthy that no correction term is needed here for determining the M–H distances, which unlike H–H distances have not been determined in solution (or in the solid state by methods other than diffraction).

Synthesis of $[\text{Mn}(\text{CO})(\text{depe})_2(\text{N}_2)][\text{BAR}'_4]$. The light yellow N_2 complex can be cleanly generated by stoichiometric reaction of NaBAR'_4 with $\text{MnBr}(\text{CO})(\text{depe})_2$ in fluorobenzene under N_2 and isolated as for the H_2 complex. $[\text{Mn}(\text{CO})(\text{depe})_2(\text{N}_2)][\text{BAR}'_4]$ will lose N_2 readily when solutions or the solid are placed under vacuum. Precautions similar to those used for the isolation of the H_2 complex must be observed to prevent degradation by oxygen. ^1H NMR in $\text{C}_6\text{D}_5\text{F}$ displayed two resonances, δ 8.32 and δ 7.64, typical for the anion and a multiplet δ 1.7–0.9 which was resolved into four major overlapping components at 500 MHz. $^{31}\text{P}\{\text{H}\}$ NMR in $\text{C}_6\text{D}_5\text{F}$ yielded only one resonance at δ 72.6 consistent with N_2 trans to CO. The $\nu(\text{CO})$ at 1896 cm^{-1} is higher in frequency than that for the agostic complex (1853 cm^{-1}), indicating that the N_2 ligand is removing electron density from the metal by π back-bonding as for H_2 and CO ligands. A strong $\nu(\text{NN})$ at 2146 cm^{-1} is lower in frequency than that for the related dppe congener (2167 cm^{-1}), which shows that the depe system possesses greater π back-bonding ability than the more electrophilic dppe system. These values are $77\text{--}96 \text{ cm}^{-1}$ higher than those for the more electron-rich Mo species.⁴

The depe complex binds N_2 completely at room temperature under 1 atm of N_2 , which contrasts sharply to the dppe complex where binding is only 37% complete.^{3a} Several other cationic complexes bind N_2 weakly or not at all, including $[\text{Mn}(\text{CO})_3(\text{PCy}_3)_2]^+$, where N_2 coordination was not seen even at $-58 \text{ }^\circ\text{C}$.^{3d} Only two ^{15}N NMR resonances (δ -30.0, Mn–NN, and δ -58.1, Mn–NN) were observed in $\text{C}_6\text{D}_5\text{F}$ for a sample enriched with 99.9% $^{15}\text{N}_2$ (Isotech) by cycling a $[\text{Mn}(\text{CO})(\text{depe})_2(\text{N}_2)][\text{BAR}'_4]$ solution in $\text{C}_6\text{D}_5\text{F}$ under vacuum and backfilling with $^{15}\text{N}_2$ several times. No ^{15}N or ^{31}P coupling was

(13) (a) Bautista, M. T.; Earl, K. A.; Maltby, P. A.; Morris, R. H.; Schweitzer, C. T.; Sella, A. *J. Am. Chem. Soc.* **1988**, *110*, 7031. (b) Desrosiers, P. J.; Cai, L.; Lin, Z.; Richards, R.; Halpern, J. *J. Am. Chem. Soc.* **1991**, *113*, 4173. (c) Crabtree, R. H. *Angew. Chem., Int. Ed. Engl.* **1993**, *32*, 789.

(14) La Placa, S. J.; Hamilton, W. C.; Ibers, J. A. *Inorg. Chem.* **1969**, *8*, 1928.

observed in the ^{15}N NMR owing to the broadening from coupling to the 5/2 spin of ^{55}Mn . However, the observation of only two ^{15}N resonances indicates that N_2 is exclusively terminally bound in solution.

Competition binding studies were carried out to examine the relative binding ability of H_2 versus N_2 . When samples of $[\text{Mn}(\text{CO})(\text{depe})_2][\text{BAR}'_4]$ and $[\text{Mn}(\text{CO})(\text{dppe})_2][\text{BAR}'_4]$ were placed under a 1:1 mixture of H_2 and N_2 , only the presence of the H_2 complex was detected by ^{31}P NMR for both systems, indicating that H_2 binds more strongly than N_2 . This is consistent with the observed equilibrium binding properties of H_2 and N_2 in the dppe system, where N_2 is only 37% bound to Mn as compared to 100% for H_2 . The result for the depe system could possibly be strictly the result of kinetics. This was tested by placing a sample of $[\text{Mn}(\text{CO})(\text{depe})_2(\text{N}_2)]^+$ under an atmosphere of H_2 by evacuating He from the headspace over the solution of the complex and backfilling with H_2 . Care was taken to evacuate the He from the headspace over the sample only after the $\text{C}_6\text{D}_5\text{F}$ solvent was frozen to avoid dissociation of N_2 . On warming and allowing the solution to stand under H_2 for several minutes, only the resonance for the H_2 complex was observed by ^{31}P NMR. This direct replacement of the N_2 ligand by H_2 confirms that H_2 is bound more strongly than N_2 in the depe system, i.e., a thermodynamic rather than kinetic control. This result is in accord with thermodynamic data observed for the $\text{Cr}(\text{CO})_3(\text{PCy}_3)_2(\text{L})$ system¹⁵ for $\text{L} = \text{H}_2, \text{N}_2$ and also the general observation that H_2 is a better ligand than N_2 on cationic complexes.^{3d}

Synthesis of $[\text{Mn}(\text{CO})(\text{SO}_2)(\text{dppe})_2][\text{BAR}'_4]$. The reaction of $\text{MnBr}(\text{CO})(\text{dppe})_2$ and $\text{Na}[\text{BAR}'_4]$ in CH_2Cl_2 at -78°C in the presence of excess SO_2 followed by warming to room temperature gave an orange solution. The latter readily lost SO_2 as evidenced by the formation of the blue color of the agostic complex and had to be maintained under an SO_2 atmosphere. An orange solid could be isolated by removing the solvent completely and placing the residue under an atmosphere of SO_2 . The proton NMR was similar to that of the H_2 complex, and $^{31}\text{P}\{^1\text{H}\}$ NMR showed a singlet at δ 67.63. The solid loses SO_2 under a He atmosphere and is partly disassociated in solution at room temperature, as observed by ^{31}P NMR which showed a signal for the agostic complex at δ 82.14. The ratio of agostic to SO_2 complex was found to be 1:6. Full coordination can be achieved by placing the solution under an atmosphere of SO_2 . Trace impurities of O_2 and SO_3 in the commercial SO_2 resulted in partial oxidation of the agostic complex yielding a contaminant of the dicarbonyl, $\text{Mn}(\text{CO})_2(\text{dppe})_2[\text{BAR}'_4]$, as identified by a ^{31}P resonance at δ 78.35. The identity of this complex was confirmed by separate generation in an NMR tube by placing a sample of $[\text{Mn}(\text{CO})(\text{dppe})_2][\text{BAR}'_4]$ under CO in $\text{C}_6\text{D}_5\text{F}$ and observing a $^{31}\text{P}\{\text{H}\}$ signal at δ 78.43. The level of impurity of dicarbonyl in the material isolated from the bulk reaction was determined to be 16% by ^{31}P NMR of a sample under a He atmosphere. Addition of SO_2 to the NMR sample increases the level of the dicarbonyl impurity. The instability of the SO_2 complex hindered determination of infrared frequencies and X-ray diffraction studies. It is conceivable that the SO_2 is coordinated here via oxygen atom(s) as in complexes with strong main group and metal Lewis acids rather than through $\eta^1\text{-S}$ or $\eta^2\text{-S,O}$ geometries.¹⁶

Table 2. Selected Bond Length (\AA) and Angle (deg) Data for $[\text{Mn}(\text{CO})(\text{LL})_2]^+$

bond (dppe)	LL = dppe	LL = depe	bond (depe)
Mn–P(1)	2.278(2)	2.275(3)	Mn–P(2)
Mn–P(2)	2.280(2)	2.275(3)	Mn–P(2a)
Mn–P(3)	2.321(2)	2.265(3)	Mn–P(1a)
Mn–P(4)	2.335(2)	2.265(3)	Mn–P(1)
Mn–CO	1.733(7)	1.72(2)	Mn–CO
C–O	1.173(8)	1.17(2)	C–O
Mn \cdots C(12)	3.456(4)	3.44(1)	Mn \cdots C(14)
Mn \cdots C(18)	3.589(4)	3.78(1)	Mn \cdots C(19)
Mn \cdots H(12)	2.89(6)	3.42 ^a	Mn \cdots H(14)
Mn \cdots H(18)	2.98(6)	3.30 ^a	Mn \cdots H(19)

angle (dppe)	LL = dppe	LL = depe	angle (depe)
P(1)–Mn–P(4)	82.67(7)	84.14(8)	P(1a)–Mn–P(2a)
P(2)–Mn–P(3)	82.90(7)	84.14(8)	P(1)–Mn–P(2)
P(1)–Mn–P(3)	95.68(7)	95.52(8)	P(1a)–Mn–P(2)
P(2)–Mn–P(4)	98.02(7)	95.52(8)	P(1)–Mn–P(2a)
P(1)–Mn–P(2)	176.75(8)	173.7(2)	P(1)–Mn–P(1a)
P(3)–Mn–P(4)	166.61(7)	174.0(2)	P(2)–Mn–P(2a)
P(1)–Mn–CO	92.3(2)	93.2(1)	P(1a)–Mn–CO
P(2)–Mn–CO	90.8(2)	93.2(1)	P(1)–Mn–CO
P(3)–Mn–CO	96.1(2)	93.0(1)	P(2)–Mn–CO
P(4)–Mn–CO	97.2(2)	93.0(1)	P(2a)–Mn–CO
Mn–P(3)–C(31)	112.1(2)	117.7(5)	Mn–P(2)–C(18)
Mn–P(2)–C(13)	115.1(2)	113.3(5)	Mn–P(1)–C(14)

^a Calculated from idealized position.

X-ray Structure of $[\text{Mn}(\text{CO})(\text{depe})_2][\text{Ga}(\text{C}_6\text{F}_5)_4]$. X-ray diffraction studies of $[\text{Mn}(\text{CO})(\text{depe})_2]^+$ with the $[\text{Ga}(\text{C}_6\text{F}_5)_4]^-$ counterion were performed. Crystals were generated by syringing fluorobenzene onto $\text{MnBr}(\text{CO})(\text{depe})_2$ and $\text{Li}[\text{Ga}(\text{C}_6\text{F}_5)_4]$, agitating the mixture vigorously, and layering hexane on top of the resulting deep blue solution. The structure showed that both the anion and cation lie on a 2-fold rotation axis which runs through the Mn and both atoms of the carbonyl. The chiral space group is consistent with the two chiral phosphorus centers. The two chiral phosphorus atoms are trans, and the enantiomer would contain the other two phosphorus atoms in analogous chiral relationship. It is interesting that the enantiomer is resolved in this structure and not in two dppe analogue structures containing either the BAR'_4^- anion^{3a} or the $[\text{Cl}(\text{Ga}(\text{C}_6\text{F}_5)_3)_2]^-$ anion (unpublished work). Both of these structures are racemic mixtures and have inversion elements between the molecules.

The coordination spheres about Mn for the depe and dppe complexes are quite similar (Table 2, Figures 1 and 2). Both systems consist of a distorted square pyramidal structure containing remote Mn \cdots H–C interactions between the phosphine organo substituents and the metal center. Unfortunately, unlike for the dppe congener, the hydrogens were not located in $[\text{Mn}(\text{CO})(\text{depe})_2]^+$, and idealized positions for them were calculated. For the dppe complex, two weak agostic interactions were located,^{3a} but for the depe analogue, the distances to four C–H bonds are much longer, especially to the calculated hydrogen positions ($>3.3 \text{\AA}$). This indicates little if any agostic interaction (see Discussion).

X-ray Structures of $[\text{Mn}(\text{CO})(\text{depe})_2(\text{H}_2)][\text{Ga}(\text{C}_6\text{F}_5)_4]$ and $[\text{Mn}(\text{CO})(\text{dppe})_2(\text{H}_2)][\text{Cl}(\text{Ga}(\text{C}_6\text{F}_5)_3)_2]$. X-ray quality crystals of $[\text{Mn}(\text{CO})(\text{depe})_2(\text{H}_2)][\text{Ga}(\text{C}_6\text{F}_5)_4]$ were grown by layering hexane over a fluorobenzene solution of the complex under H_2 . Attempts to prepare crystals of the BAR'_4 analogue resulted in twinned crystals. The cation is an octahedral complex (Figure 3, Table 3) that contains an H_2 ligand trans to CO similar to the structure of the Mo analogue $\text{Mo}(\text{CO})(\text{depe})_2(\text{H}_2)$.^{4a} Electron density for the H_2 was found in appropriate locations but could not be refined and was not included in the final refinement.

(15) Gonzalez, A. A.; Hoff, C. D. *Inorg. Chem.* **1989**, *28*, 4295.

(16) (a) Ryan, R. R.; Kubas, G. J.; Moody, D. C.; Eller, P. G. *Struct. Bonding (Berlin)* **1981**, *46*, 47. (b) Kubas, G. J. *Acc. Chem. Res.* **1994**, *27*, 183.

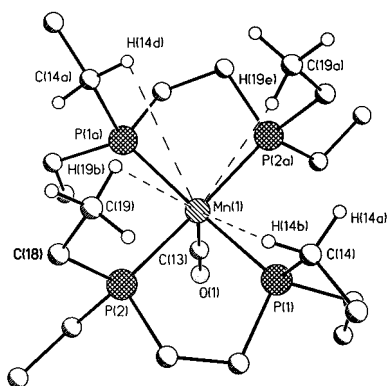
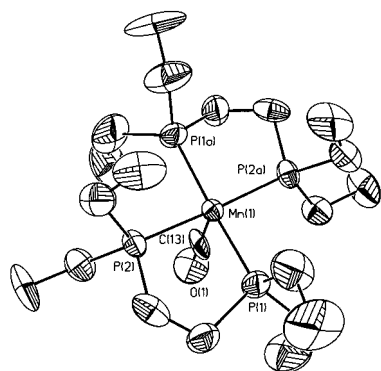


Figure 1. ORTEP diagram for the cation of $[\text{Mn}(\text{CO})(\text{depe})_2][\text{Ga}(\text{C}_6\text{F}_5)_4]$ (50% probability ellipsoids) and ball-and-stick drawing showing idealized hydrogen positions with closest $\text{M}\cdots\text{H}$ separations.

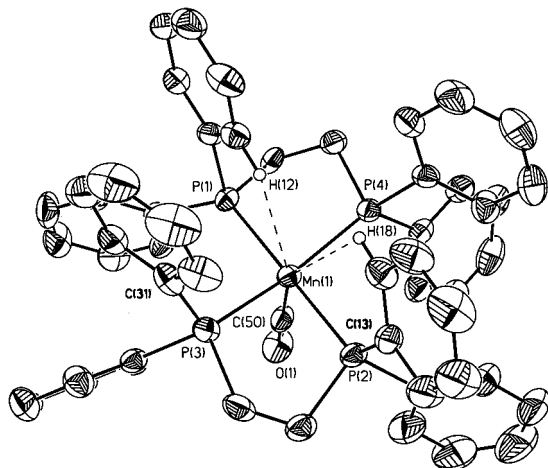


Figure 2. ORTEP diagram for the cation of $[\text{Mn}(\text{CO})(\text{dppe})_2][\text{Ga}(\text{C}_6\text{F}_5)_4]$ (50% probability ellipsoids).

Table 3. Selected Bond Length (\AA) and Angle (deg) Data for $[\text{Mn}(\text{CO})(\text{depe})_2(\text{H}_2)][\text{Ga}(\text{C}_6\text{F}_5)_4]$

Mn–P(1)	2.292(1)	Mn–P(4)	2.269(1)
Mn–P(2)	2.291(2)	Mn–CO	1.777(4)
Mn–P(3)	2.271(1)	C–O	1.139(5)
P(1)–Mn–P(2)	84.15(4)	P(2)–Mn–P(4)	178.29(5)
P(3)–Mn–P(4)	85.40(4)	P(1)–Mn–CO	90.69(13)
P(2)–Mn–P(3)	95.69(4)	P(2)–Mn–CO	92.51(14)
P(1)–Mn–P(4)	94.78(4)	P(3)–Mn–CO	88.44(13)
P(1)–Mn–P(3)	179.11(4)	P(4)–Mn–CO	88.83(15)

$[\text{Mn}(\text{CO})(\text{dppe})_2(\text{H}_2)][\text{BAR}'_4]$ gave twinned crystals. In an attempt to grow crystals of the $[\text{Ga}(\text{C}_6\text{F}_5)_4]^-$ salt by layering hexane over a CH_2Cl_2 solution under H_2 , crystals of $[\text{Mn}(\text{CO})(\text{dppe})_2(\text{H}_2)][\text{Cl}(\text{Ga}(\text{C}_6\text{F}_5)_4)_2]$ were isolated with a chloride-bridged Ga anion. The agostic complex from which the H_2

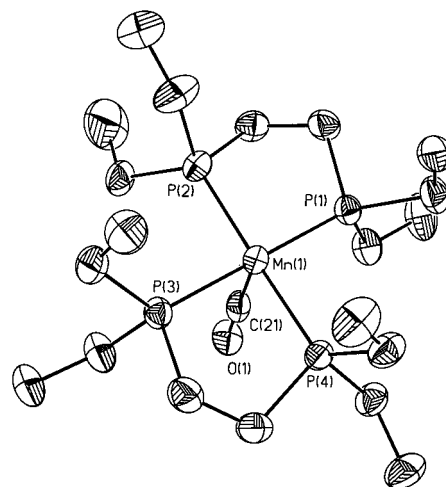


Figure 3. ORTEP diagram for the cation of $[\text{Mn}(\text{CO})(\text{depe})_2(\text{H}_2)][\text{Ga}(\text{C}_6\text{F}_5)_4]$ (50% probability ellipsoids).

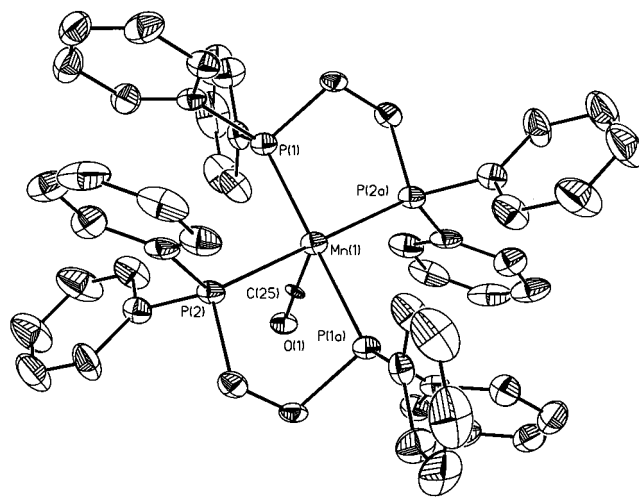


Figure 4. ORTEP diagram for the cation of $[\text{Mn}(\text{CO})(\text{dppe})_2(\text{H}_2)][\text{Cl}(\text{Ga}(\text{C}_6\text{F}_5)_3)_2]$ (50% probability ellipsoids).

Table 4. Selected Bond Length (\AA) and Angle (deg) Data for $[\text{Mn}(\text{CO})(\text{dppe})_2(\text{H}_2)][\text{Cl}(\text{Ga}(\text{C}_6\text{F}_5)_3)_2]$

Mn–P(1)	2.308(2)	Mn–CO	1.839(12)
Mn–P(2)	2.324(2)		
P(1)–Mn–P(2)	96.50(7)	P(1a)–Mn–CO	84.6(4)
P(1a)–Mn–P(2)	83.50(7)	P(2)–Mn–CO	87.7(4)
P(1)–Mn–P(1a)	180.0	P(2a)–Mn–CO	92.3(4)
P(1)–Mn–CO	95.4(4)		

complex was prepared was synthesized from $\text{LiGa}(\text{C}_6\text{F}_5)_4$ that contained a chloride impurity as determined by a AgNO_3 test. Although ^{19}F NMR revealed the presence of greater amounts of fluorocarbon impurities as compared to other syntheses of $\text{LiGa}(\text{C}_6\text{F}_5)_4$, the major product was identified to be the anion $[\text{Ga}(\text{C}_6\text{F}_5)_4]^-$. ^{13}C NMR of this material indeed revealed only the presence of $[\text{Ga}(\text{C}_6\text{F}_5)_4]^-$. However, the dinuclear chloride-bridged anion, $[\text{Cl}(\text{Ga}(\text{C}_6\text{F}_5)_3)_2]^-$, was present in sufficient quantity to selectively crystallize with the $[\text{Mn}(\text{CO})(\text{dppe})_2(\text{H}_2)]^+$ cation (Figure 4, Table 4). Electron density for the H_2 was not located because of disorder between the H_2 and trans-CO ligands.

X-ray Structures of $[\text{Ga}(\text{C}_6\text{F}_5)_4]^-$ and $[\text{Cl}(\text{Ga}(\text{C}_6\text{F}_5)_3)_2]^-$. Structural data for the anion of $[\text{Mn}(\text{CO})(\text{depe})_2(\text{H}_2)][\text{Ga}(\text{C}_6\text{F}_5)_4]$ are given in Figure 5 and Table 5 and can be compared to that for similar Ga compounds.¹⁷ The Ga in $[\text{Ga}(\text{C}_6\text{F}_5)_4]^-$ is tetrahedrally coordinated, although distorted from ideal geom-

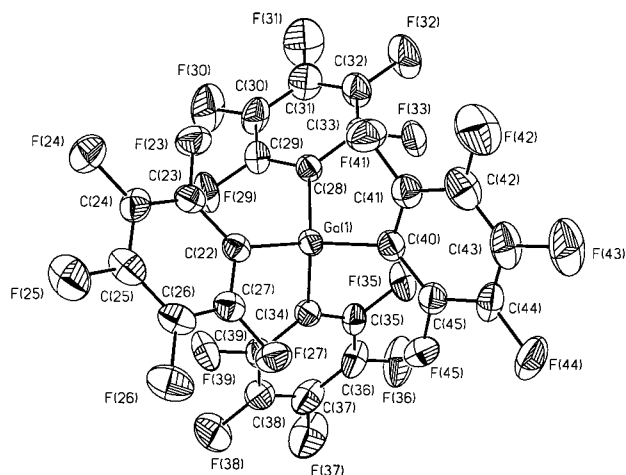


Figure 5. ORTEP diagram for $[\text{Ga}(\text{C}_6\text{F}_5)_4]^-$ (50% probability ellipsoids).

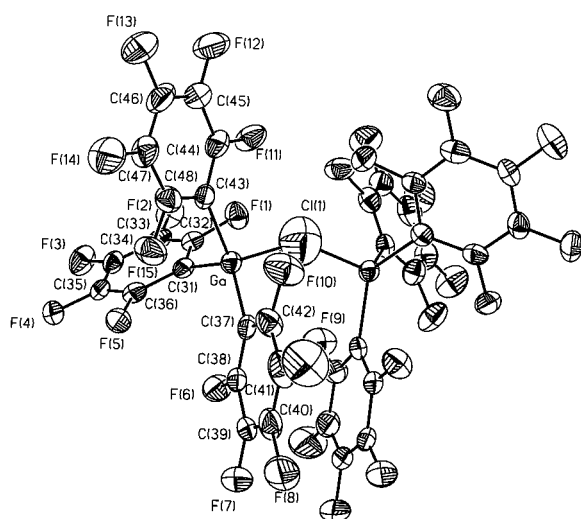


Figure 6. ORTEP diagram for $[\text{Cl}\{\text{Ga}(\text{C}_6\text{F}_5)_3\}_2]^-$ (35% probability ellipsoids).

Table 5. Selected Bond Length (Å) and Angle (deg) Data for the $[\text{Ga}(\text{C}_6\text{F}_5)_4]^-$ Anion in $[\text{Mn}(\text{CO})(\text{depe})_2(\text{H}_2)][\text{Ga}(\text{C}_6\text{F}_5)_4]$

Ga—C(22)	2.011(4)	Ga—C(34)	2.015(4)
Ga—C(28)	2.014(6)	Ga—C(40)	2.005(4)
C(22)—Ga—C(40)	101.5(2)	C(22)—Ga—C(28)	115.7(2)
C(28)—Ga—C(40)	113.1(2)	C(34)—Ga—C(28)	102.2(2)
C(34)—Ga—C(40)	112.6(2)	C(22)—Ga—C(34)	112.1(2)

etry. This structure is similar to that for the anion in $\text{K}[\text{Ga}(\text{CH}_3)_4]$, which is a distorted tetrahedron possessing a Ga—C distance of 2.31(3) Å with two reported C—Ga—C angles of 81(10)° and 125(10)°. ^{17a} The shortening of the Ga—C distances in $[\text{Ga}(\text{C}_6\text{F}_5)_4]^-$ is the result of the change from an electron rich CH_3 group to the electron-deficient C_6F_5 group. The distances in $[\text{Ga}(\text{CH}_3)_4]^-$ are much more closely related to those in the neutral $\text{Ga}(\text{C}_6\text{H}_5)_3$ (Ga—C = 1.946(7), 1.968(5)). ^{17b}

Structural data for the anion in $[\text{Mn}(\text{CO})(\text{dppe})_2(\text{H}_2)][\text{Cl}\{\text{Ga}(\text{C}_6\text{F}_5)_3\}_2]^-$ are given in Figure 6 and Table 6. The Ga atoms in $[\text{Cl}\{\text{Ga}(\text{C}_6\text{F}_5)_3\}_2]^-$ are tetrahedrally coordinated by three C_6F_5 groups and a bridging Cl. Metrical data indicate that the

Table 6. Selected Bond Length (Å) and Angle (deg) Data for the $[\text{Cl}\{\text{Ga}(\text{C}_6\text{F}_5)_3\}_2]^-$ Anion in $[\text{Mn}(\text{CO})(\text{dppe})_2(\text{H}_2)][\text{Cl}\{\text{Ga}(\text{C}_6\text{F}_5)_3\}_2]^-$

Ga—Cl(1)	1.925(3)	Ga—C(37)	1.986(8)
Ga—C(31)	2.002(8)	Ga—C(43)	2.003(8)
Cl(1)—Ga—C(31)	106.2(2)	C(37)—Ga—C(43)	112.2(3)
Cl(1)—Ga—C(37)	104.9(3)	C(31)—Ga—C(43)	106.2(3)
Cl(1)—Ga—C(43)	104.4(3)	Ga—Cl(1)—Ga#2	138.9(5)
C(37)—Ga—C(31)	121.6(3)		

Table 7. Comparison of Metal—Agostic Distances

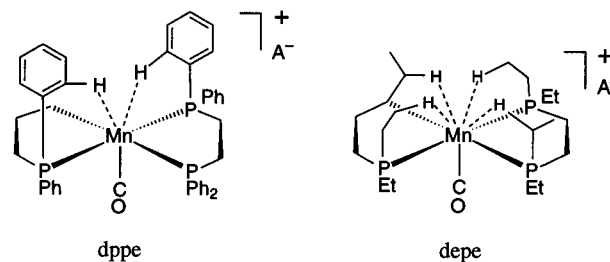
complex	$\text{M}\cdots\text{H}$, ^a Å	$\text{M}\cdots\text{C}$, Å
$\text{Cr}(\text{CO})_3(\text{PCy}_3)_2$	2.240(1)	2.884(1)
$\text{Mo}(\text{CO})(\text{dppe})_2$	2.98(11)	3.50(2)
$\text{Mo}(\text{CO})(\text{dBu}^i\text{pe})_2$	2.20	3.007(4)
$\text{W}(\text{CO})_3(\text{PCy}_3)_2$	2.27	2.945(6)
$[\text{Mn}(\text{CO})(\text{dppe})_2]^+$	2.89(6), 2.98(6)	3.456(4), 3.589(4)
$[\text{Mn}(\text{CO})_3(\text{PCy}_3)_2]^+$	2.01(9)	2.75(3) ^b
$[\text{Re}(\text{CO})_3(\text{PCy}_3)_2]^+$		2.89(5)
$[\text{Ru}(\text{Ph})(\text{CO})(\text{P}^i\text{Bu}_2\text{Me})_2]^+$		2.87, 2.88
$[\text{IrH}_2(\text{P}^i\text{Bu}_2\text{Ph})_2]^+$		2.81—2.94 ^c

^a Idealized $\text{M}\cdots\text{H}$ if no esd's given. ^b Average value for disordered carbons. ^c For three independent molecules with two agostic interactions each.

geometry around Ga is distorted from ideal symmetry. The geometry about the Cl atom reveals that the Ga centers adopt a bent geometry, which can be rationalized by repulsion of lone pairs on the Cl. The Ga—C distances in $[\text{Cl}\{\text{Ga}(\text{C}_6\text{F}_5)_3\}_2]^-$ are comparable to those in $[\text{Ga}(\text{C}_6\text{F}_5)_4]^-$ and shorter than that in $[\text{GaCl}(\text{CH}_3)_3]^-$ (2.381 Å) ^{17a} as a result of Ga being coordinated to the electron-deficient $\text{Ga}(\text{C}_6\text{F}_5)_3$ fragment. Although no other X-ray diffraction data could be located for compounds of the form $[\text{R}_3\text{Ga—X—GaR}_3]^-$, IR and Raman data suggest a structure with C_{2v} symmetry for complexes where X is Cl or Br. ¹⁸

Discussion

Polyagostic Interactions in $[\text{M}(\text{CO})(\text{diphosphine})_2]^+ \text{Complexes}$. The geometry of the $[\text{Mn}(\text{CO})(\text{diphosphine})_2]^+$ cations is formally five-coordinate square pyramidal. The notable feature is the presence of *multiple* remote agostic interactions with the manganese center involving C—H groups located on the phenyl or ethyl substituents of the phosphines. The dppe complex

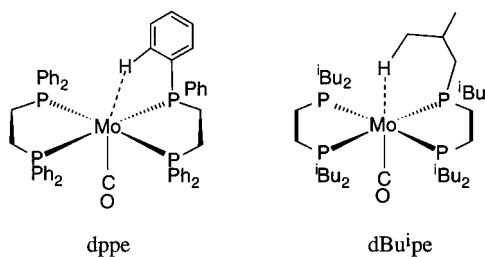


contains two weak interactions, but the depe system appears to have four C—H bonds from ethyl groups approaching the metal center, albeit at much longer distances (Table 7) suggestive of van der Waals contacts with perhaps only a small contribution from agostic binding. The Mn systems contrast with the neutral $\text{Mo}(\text{CO})(\text{diphosphine})_2$ analogues, which contain only one interaction from either an ortho phenyl C—H from dppe^{4b} or an isobutyl γ -C—H from $^i\text{Bu}_2\text{PC}_2\text{H}_4\text{P}^i\text{Bu}_2$ ($\text{d}^i\text{Bu}^i\text{pe}$). ¹⁹

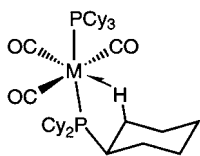
(17) (a) Maire, J.; Krueken, U.; Mirbach, M.; Petz, W.; Siebert, C. *Gemelin Handbook of Inorganic Chemistry Ga*, Part 1; Krueken, U., Mirbach, M., Petz, W., Siebert, C., Eds.; Springer-Verlag: Berlin, 1987; pp 313–336. (b) Malone, J. F.; McDonald, W. S. *J. Chem. Soc. A* **1970**, 3362.

(18) Wilson, I. L.; Dehnicke, K. *J. Organomet. Chem.* **1974**, 67, 229.

(19) Luo, X. L.; Kubas, G. J.; Burns, C. J.; Butcher, R. J.; Bryan, J. C. *Inorg. Chem.* **1995**, 34, 6538.



The very long, tenuous polyagostic Mn interactions most likely are a result of the reduced Mn–P–C–H ring size as compared to the Mo system, which prevents full interaction of the C–H bond (for the dppe system, the average Mn–P is 2.303 Å versus 2.452 Å for the larger Mo coordination sphere). For both $[\text{Mn}(\text{CO})(\text{diphosphine})_2]^+$ complexes and also the Mo-dppe analogue, the M–P–C bond angles in the chelating five-membered agostic ring were not severely contracted compared to the analogous angles for the atoms not involved in the agostic bonding. This is unlike the case for the less constrained monodentate phosphine system $\text{M}(\text{CO})_3(\text{PCy}_3)_2$ (M = Cr,²⁰ W,²¹ Re^{+10a} and Mn^{+10a}) where the metal can more strongly attract a single C–H, and Cr–P–C is 98.8° compared to ca. 120° for the equivalent angles not involved in the agostic interaction. Also, the P atom is able to bend away from normal position here (P–Cr–P = 160.2°) to facilitate closer approach of the agostic C–H. The Mn···H distances are in fact much longer



(2.89(6) and 2.98(6) Å for dppe; 3.30 and 3.42 Å calculated for each Mn···H_β and each Mn···H_α for depe) than that found for the single CH interaction in $[\text{Mn}(\text{CO})_3(\text{PCy}_3)_2]^+$ (2.01(9) Å). Table 7 compares these distances for a variety of agostic systems. The Mo···H distance is also long, 2.98(11) Å, in $\text{Mo}(\text{CO})(\text{dppe})_2$,^{4b} although it must be kept in mind that Mo is a larger second-row metal. On the other hand, for $\text{Mo}(\text{CO})(\text{dBu}^i\text{-pe})_2$, the calculated Mo···H distance is much shorter, 2.20 Å, and the Mo–P–C angle in the chelate ring (six-membered here) is somewhat contracted (113.0° relative to the other Mo–P–C angles of the same type (122.8° avg)). It is not clear why the interaction is significantly stronger here than in the other Mo and Mn diphosphine systems, although the six-membered ring may bring the C–H bond closer to the metal with less overall bond strain than for a five-membered ring. The agostic hydrogen lies more directly trans to the CO (H···Mo–C = 166.0°) than for $\text{Mo}(\text{CO})(\text{dppe})_2$ or the Mn species, where the H···Mo–C angles are much more acute. This angle is even closer to linear (173.1°) in $\text{Cr}(\text{CO})_3(\text{PCy}_3)_2$.

The M···C distances also reflect the relative strengths of the agostic interactions. For $\text{Mo}(\text{CO})(\text{dBu}^i\text{-pe})_2$ it is 3.007(4) Å, much shorter than that in the dppe congener (3.50(2) Å) and those in the Mn cations but significantly longer than in the majority of cases. For $[\text{Mn}(\text{CO})(\text{dppe})_2]^+$ the distances are 3.456(4) and 3.589(4) Å, and for the depe analogue they are 3.44(1) for each M···C_α and 3.78(1) Å for each M···C_β, very

long in all cases. Only a maximum total of 2e from the agostic interactions need to be donated to these 16e fragments, so each individual interaction represents donation of much less than 2e from each C–H bond. These complexes thus accommodate approach of available nearby electron density with the minimum amount of distortion of their octahedral stereochemistry, even if the metal can only receive small bits from several sources.

Although polyagostic interactions have been observed in several systems,^{22,23} those involving phosphine C–H bonds are still rare. A 4-fold interaction (two M–P–*ortho*-phenyl-H and two M–*tert*-butyl-H) exists in the formally 14e complexes $\text{M}(\text{PPhBu}^t)_2$ (M = Pt, Pd; M···H estimated to be 2.5–2.6 Å).^{22a} A more recent and relevant example is 14e $[\text{Ru}(\text{Ph})(\text{CO})(\text{PBu}^t\text{-Me})_2]^+$ with two agostic Ru···H–C interactions originating from one *tert*-Bu substituent on each phosphine.^{22b} The preference for donation from *tert*-Bu over Me substituents is attributed to better steric approach of the former (giving a five-membered ring) than the latter (four-membered). The Ru–C distances are quite short, 2.87 and 2.88 Å, indicative of strong agostic interactions²³ to the more highly unsaturated 14e fragment (the polyagostic bonding to Mn involves less-unsaturated 16e fragments). Related 14e $[\text{IrH}_2(\text{PBu}^t\text{Ph})_2]^+$ also shows two strong interactions, but an *ortho*-metalated analogue gives only one.^{22e,f} 16e $[\text{IrH}_2(\text{PCy}_2\text{Ph})_3]^+$ gives one agostic interaction, but the less bulky PPr^i_2Ph analogue shows only very distant M···C (e.g., 3.46 Å) as for the Mn–diphosphine system. Steric factors are thus clearly of major importance in agostic phosphine systems, as also shown computationally.^{22e,f} The proximity (or unstrained approachability) of C–H bonds to the metal is obviously critical to the strength and/or number of interactions.

Relative Electrophilicity of Cationic Versus Neutral Fragments and Correlation of CO Stretching Frequencies and Bond Lengths with π -Acceptor Strengths of *trans* Ligands.

To assess the activation of H₂ and other π -acceptor ligands on a series of related complexes, IR frequencies and metrical data for the CO ligand *trans* to the ligand of interest are correlated in Table 8. The variations include metal, ligand, and charge on the complex. Clearly the Mn(I) cations have the highest $\nu(\text{CO})$, about 100 cm⁻¹ higher than the corresponding Mo(0) species, demonstrating the much higher electrophilicity of cations and the consequent reduced back-bonding to CO that raises $\nu(\text{CO})$. The recently reported *dicationic* complex $[\text{Fe}(\text{H}_2)(\text{CO})(\text{dppe})_2]^{2+}$ has a far higher $\nu(\text{CO})$, 2006 cm⁻¹,^{5a} than any complex in Table 8. This value is 110 cm⁻¹ higher yet than that for the monocationic Mn⁺ congener, emphasizing that the charge on the complex is the dominant factor here, much more than the basicity of the *cis*-phosphine coligands. In the H₂ and N₂ adducts, $\nu(\text{CO})$ for the depe and dBuⁱpe systems are only ca. 10–30 cm⁻¹ lower than for the dppe species. This is less than may have been expected for substituting four trialkylphosphine ligands by four diarylalkylphosphine donors, but it is consistent with the effect in $\text{MnBr}(\text{CO})(\text{diphosphine})_2$. The difference is even less in the cationic Mn species than in the Mo complexes (15 vs 32 cm⁻¹ for N₂ adducts), reflecting the leveling effect

(20) Zhang, K.; Gonzalez, A. A.; Mukerjee, S. L.; Chou, S.-J.; Hoff, C. D.; Kubat-Martin, K. A.; Barnhart, D.; Kubas, G. J. *J. Am. Chem. Soc.* **1991**, *113*, 9170.
(21) Wasserman, H. J.; Kubas, G. J.; Ryan, R. R. *J. Am. Chem. Soc.* **1986**, *108*, 2294.

(22) (a) Otsuka, S.; Yoshida, T.; Matsumoto, M.; Nakatsu, K. *J. Am. Chem. Soc.* **1976**, *98*, 588. (b) Huang, D.; Streib, W. E.; Eisenstein, O.; Caulton, K. G. *Angew. Chem., Int. Ed. Engl.* **1997**, *36*, 2004. (c) Cole, J. M.; Gibson, V. C.; Howard, J. A. K.; McIntyre, G. J.; Walker, G. L. *P. Chem. Commun.* **1998**, 1829. (d) Evans, W. J.; Anwender, R.; Ziller, J. W.; Khan, S. I. *Inorg. Chem.* **1995**, *34*, 5927. (e) Cooper, A. C.; Clot, E.; Huffman, J. C.; Streib, W. E.; Maseras, F.; Eisenstein, O.; Caulton, K. G. *J. Am. Chem. Soc.* **1999**, *121*, 97. (f) Ujaque, G.; Cooper, A. C.; Maseras, F.; Eisenstein, O.; Caulton, K. G. *J. Am. Chem. Soc.* **1998**, *120*, 361.
(23) Braga, D.; Grepioni, F.; Biradha, K.; Desiraju, G. R. *J. Chem. Soc., Dalton Trans.* **1996**, 3925.

Table 8. Comparison of $\nu(\text{CO})$ and CO Bond Lengths in Adducts of d^6 Fragments with Ligands of Varying π -Acceptor Strength Trans to CO

metal fragment	ligand	$\nu(\text{CO}), \text{cm}^{-1}$	C—O, Å	M—C, Å	ref
[Mn(CO)(dppe) ₂] ⁺	agostic	1839	1.173(8)	1.733(7)	3a
	H ₂	1896	1.16(2)	1.839(12)	3a
	N ₂	1911			3a
[Mn(CO)(depe) ₂] ⁺	“agostic”	1853	1.17(2)	1.72(2)	this work
	H ₂	1887	1.139(5)	1.777(4)	this work
	N ₂	1896			this work
	CO	1888			this work
Mo(CO)(dppe) ₂	NH ₃	1709			43
	agostic	1723	1.192(12)	1.903(9)	4
	H ₂	1814	1.179(6)	1.933(5)	4a
	N ₂	1809	1.127(20)	1.973(16)	4b
Mo(CO)(dBu ⁱ pe) ₂	agostic	1724	1.190(5)	1.886(4)	19
	N ₂	1777			4a
W(CO) ₃ (PCy ₃) ₂	H ₂ O ^a	1725	1.21(1)	1.875(8)	46
	agostic	1797	1.180(7)	1.902(6)	21
	H ₂	1843	1.17(1)	1.99(1)	42b, 47
	N ₂	1835			21
	C ₂ H ₄	1834	1.159(5)	1.977(4)	30c
	CO	1865	1.13(1) ^b	2.05(1) ^b	48
	mpz ⁺ c	1888	1.097(19)	2.055(17)	49
W(CO) ₃ (PPr ^t) ₂	I ^d	1870	1.094(13)	1.958(11)	50
	Mo(CO) ₃ (PPr ^t) ₂	SO ₂	1889	2.04(1)	51
W(CO) ₅	H ₂	1971		2.006 ^e	2b, 52
	N ₂	1961		2.013 ^e	2b, 53
	NO ⁺			2.178 ^e	2b

^a Water protons are hydrogen bonded to the axial CO ligand and also a lattice THF. ^b Average value. ^c Ligand is methylpyrazinium cation; complex is [W(mpz)(CO)₃(PCy₃)₂][PF₆]. ^d Complex is a 17-e W(I) radical; W—C distance may not correlate with those for the W(0) species. ^e Calculated.

of the positive charge. The agostic species show a reversal of this trend for Mn and little difference in $\nu(\text{CO})$ for Mo, indicating that the strength and/or number of agostic interactions may be a factor (the Mn-depe complex has virtually no agostic contribution).

The recently reported⁶ H₂ complexes with phosphite donors, [Mn(H₂)(CO)P₄][BPh₄] (P = P(OEt)₃, PPh(OEt)₂) have higher $\nu(\text{CO})$ values (1926 cm⁻¹) than any of the complexes in Table 8, indicating that they are significantly more electron poor than the corresponding bidentate phosphine complexes where $\nu(\text{CO})$ is 30 cm⁻¹ lower. The complexes resulting from dissociation of H₂ from [Mn(H₂)(CO)P₄][BPh₄] are claimed to have agostic interactions on the basis of ³¹P NMR evidence. However, unlike our phosphine complexes, there is a glaring disparity in the reported $\nu(\text{CO})$ values in the solid state for the P(OEt)₃ (1872 cm⁻¹) and PPh(OEt)₂ (1915 cm⁻¹) species. Furthermore, the small difference between the latter value and that for the corresponding H₂ complex (1926 cm⁻¹) is far less than those for other systems with agostic versus H₂ ligands. Finally, the yellow color of the isolated products of H₂ removal conflicts with the characteristic intense blue color of the agostic Mn and Mo diphosphine systems. Because the BPh₄ anion is more likely to interact with the metal than BAR'₄, and a coordinating solvent (ethanol) was used in isolating the solids, it is conceivable that the solid phosphite complexes have anion or solvent interactions rather than agostic interactions. The three ³¹P NMR signals reported for {Mn(H₂)(CO)[P(OEt)₃]₄}[BPh₄] in CH₂Cl₂ solution at 183 K might result from a mixture of agostic and solvento forms (CH₂Cl₂ coordinates^{3c} to Re(CO)₄(PR₃)⁺). It should be noted that for [Mn(CO)(dppe)₂][BAR'₄], only one ³¹P signal was observed down to 198 K in CD₂Cl₂ because of the high fluxionality of the agostic interactions.^{3a}

The IR data and also C—O and M—C bond lengths can also be used to gauge the π -acceptor strengths of ligands trans to the CO because of the well-known trans effect. The agostic C—H bonds are the weakest ligands trans and also the weakest acceptors, and the influence on $\nu(\text{CO})$ is similar to that for pure

σ donors such as NH₃. In contrast, the H₂ ligand is an excellent acceptor as strong as N₂ and ethylene, and all of the complexes with these ligands have similar $\nu(\text{CO})$ values much higher than those for the corresponding agostic complexes. As can be seen from Table 8, the C—O bond length always decreases and the M—C bond length increases substantially when acceptor ligands replace the trans agostic interactions. This effect, like the increased $\nu(\text{CO})$, is attributable primarily to reduced M → CO back-bonding because of increased competition for $d\pi$ -electron density. Theoretical calculations of the bond lengths in M(CO)₅L (M = Cr, Mo, W) also led to a similar correlation that strong acceptors L increase the M—CO_{trans} length whereas poor acceptors decrease it.^{2b} The M(CO)₃(PR₃)₂(L) complexes show the greatest range of trans-ligand effects. The longest C—O distance, 1.21(1) Å, and shortest W—C length is for the pure σ -donating H₂O adduct, although there is intermolecular hydrogen bonding between CO and H₂O that might weaken the C—O bond. The $\nu(\text{CO})$ value is 1725 cm⁻¹, the lowest by far in the W(L)(CO)₃(PCy₃)₂ series. At the other end of the spectrum are complexes with powerful π acceptors such as CO, SO₂, and mpz⁺ (methylpyrazinium), which have C—O in the 1.09–1.13 Å range and $\nu(\text{CO})$ at 1865–1889 cm⁻¹. Also in this group is WI(CO)₃(PPr^t)₂, which is a W^I radical with a less electron-rich 17e metal center. The H₂, N₂, and ethylene ligands give intermediate parameters, indicating they are not quite as strongly π -accepting as CO and SO₂.

Inelastic Neutron Scattering Studies of [Mn(CO)-(diphosphine)₂(H₂)]⁺. Considerable insight into metal—H₂ interactions has been obtained by studying the barrier to rotation of coordinated H₂ by inelastic neutron scattering (INS) techniques.²⁴ This barrier arises primarily from the variation in the back-bonding interaction between $d\pi(\text{M})$ and the $\sigma^*(\text{H}_2)$ orbitals as the H₂ ligand is rotated around the σ bond to the metal.

(24) (a) Eckert, J.; Kubas, G. J. *J. Phys. Chem.* **1993**, *97*, 2378. (b) Taylor, A. D.; Wood, E. J.; Goldstone, J. A.; Eckert, J. *Nucl. Instrum. Methods Phys. Res.* **1984**, *221*, 408. (c) Eckert, J. *Spectrochim. Acta* **1992**, *48A*, 363. (d) Eckert, J. *Physica* **1986**, *136B*, 150. (e) Albinati, A.; Klooster,

Table 9. Tunneling Frequency, ω_t (cm^{-1}), Observed and Calculated Rotational Transitions, τ (cm^{-1}), Barrier Heights, V_n (kcal/mol), and $\delta(\text{Mn}(\text{H}_2))$, i.e., Wag or Rock, for Dihydrogen in $[\text{Mn}(\text{CO})(\eta^2\text{-H}_2)\text{L}_2]^+$, L = dppe, depe^a

	L			
	dppe, $B = 41$		depe, $B = 43$	
	obs	calcd	obs	calcd
		$V_2 = 1.22$ $V_4 = -0.11$		$V_2 = 1.17$ $V_4 = -0.15$
ω_t	4(1)	3.3		4.2
τ	188, 218	186, 223	178, 212	178, 219
	332	329	315	322
$\delta(\text{Mn}(\text{H}_2))$	422		390	
$\delta(\text{Mn}(\text{H}_2))$	580		535	

^a Uncertainties in the frequencies are approximately 2% of their value.

Therefore, the barrier height, derived from measurements of the rotational transitions, provides an indication of the relative strength of the back-bonding interaction. INS measurements of the rotational and vibrational transitions of the H_2 ligand for both the dppe and depe congeners were performed to determine the rotational barriers and relate them to other data concerning the nature of the $\text{M}-\text{H}_2$ bonding in these compounds.

The rotational tunneling lines for $[\text{Mn}(\text{CO})(\text{H}_2)(\text{dppe})_2]^+$ were extremely broad and poorly defined in the same manner as was recently reported^{24e} for $[\text{RuH}(\text{H}_2)(\text{dppe})_2]^+$ but unlike those observed for most other H_2 complexes that do not have the fairly symmetric diphosphine ligands. The reason for this observation must lie in the fact that the Mn center is nearly coplanar with the four P atoms for both of the present complexes, with the result that the rotational potential wells have very flat bottoms. At low temperatures, this would give rise to an inhomogeneous broadening of the rotational tunneling lines because the equilibrium position for this potential is not well defined in the presence of the large zero-point vibrational amplitude of the H_2 ligand. The observed rotational tunneling band position, as well as the torsional and some vibrational frequencies, are presented in Table 9.

Barrier heights were computed in the same manner previously reported²⁴ with values of the rotational constant B (calculated here from the NMR-derived $\text{H}-\text{H}$ distances) held fixed at 41 and 43 cm^{-1} for the dppe and depe complexes, respectively. The barrier heights derived in this fashion, along with the calculated values of the rotational transitions, are also given in Table 9. The results for the rotational transitions and associated barrier heights for both compounds are found to be rather similar, in accord with the fact that the degree of $\text{H}-\text{H}$ bond activation as measured by $d(\text{HH})$ is similar. Differences in the frequencies of the rocking and wagging modes are more pronounced. This may in part be related to differences in mixing of these vibrations with skeletal motions that would be expected to differ for the dppe and depe ligands because of the substantially different masses of phenyl and ethyl groups.

It should be noted that the rotational barriers for the dppe and depe complexes are nearly equal, ~ 1.2 kcal/mol, which indicates that the influence of the cis ligands (e.g., raising or lowering back-donation) is relatively unimportant here, as discussed below. The barriers are less than that for the related compound $[\text{FeH}(\text{H}_2)(\text{dppe})_2]^+$,^{24f} but greater than that in Mo-

Table 10. $J(\text{HD})$ Coupling Constants and $\text{H}-\text{H}$ Distances for H_2 Complexes of Various Fragments with Trans-CO Ligands

metal fragment	$J(\text{HD})$, Hz	$\text{H}-\text{H}$, Å ^a	ref
$\text{Cr}(\text{CO})_3(\text{PPr}^i_3)_2$	35	0.84–0.85	40
$\text{Cr}(\text{CO})_3(\text{PCy}_3)_2$		0.85(1) ^b	40
$\text{Mo}(\text{CO})_3(\text{PCy}_3)_2$		0.87 ^b	41
$\text{Mo}(\text{CO})(\text{dppe})_2$	34	0.88(1) ^b	4a, 41
		0.85–0.87	
$\text{Mo}(\text{CO})(\text{dBzpe})_2$	30	0.92–0.94	55
$\text{W}(\text{CO})_3(\text{PPr}^i_3)_2$ ^c	33.5	0.89(1) ^b	41, 42
		0.86–0.88	
$\text{W}(\text{CO})_3(\text{PCy}_3)_2$ ^c		0.89(1) ^b	41
$[\text{Mn}(\text{CO})(\text{dppe})_2]^+$	32	0.89(2) ^b	3a
		0.89–0.90	
$[\text{Mn}(\text{CO})(\text{depe})_2]^+$	33	0.87–0.89	this work
$[\text{Mn}(\text{CO})(\text{P}(\text{OEt})_3)_4]^+$	32	0.89–0.90	6
$[\text{Mn}(\text{CO})(\text{PPh}(\text{OEt})_2)_4]^+$	32.5	0.88–0.89	6
$\text{Mn}(\text{CO})_2(\text{P}(\text{OEt})_3)_3]^+$	33	0.87–0.89	6
$[\text{Mn}(\text{CO})_3(\text{PCy}_3)_2]^+$	33	0.87–0.89	3d
$[\text{Re}(\text{CO})_4(\text{PPh}_3)]^+$	33.9	0.85–0.87	3c
$[\text{Re}(\text{CO})_4(\text{PCy}_3)]^+$	33.8	0.85–0.87	3c
$[\text{Re}(\text{CO})_3(\text{PCy}_3)_2]^+$	32	0.89–0.90	10c
$[\text{Re}(\text{CO})_3(\text{PPr}^i_3)_2]^+$	33	0.87–0.89	10c
$[\text{Re}(\text{CO})_3(\text{PPh}_3)_2]^+$	32	0.89–0.90	10c
$[\text{Re}(\text{CO})_3\{\text{P}(\text{OEt})_3\}_2]^+$	30	0.92–0.94	54
$[\text{Re}(\text{CO})_2(\text{PMe}_2\text{Ph})_3]^{\text{+c}}$	31	0.90–0.92	44
$[\text{Re}(\text{CO})_2\{\text{P}(\text{OEt})_3\}_3]^{\text{+c}}$	33	0.87–0.89	54
$[\text{Re}(\text{CO})\{\text{P}(\text{OEt})_3\}_4]^{\text{+c}}$	33	0.87–0.89	54
$[\text{ReH}_2(\text{CO})(\text{PMe}_3)_3]^{\text{+c}}$	33.6	0.86–0.88	45
$[\text{Fe}(\text{CO})(\text{dppe})_2]^{2+}$	33.1	0.87–0.88	5a
$[\text{Ru}(\text{CO})(\text{dppp})_2]^{2+}$	34	0.85–0.87	5b
$[\text{Os}(\text{CO})(\text{dppp})_2]^{2+}$	32	0.89–0.90	5b

^a Except where noted, calculated from and bracketed by the empirical relationships, $r_{\text{HH}} = 1.42 - 0.0167J(\text{HD})$ (ref 12a) and $r_{\text{HH}} = 1.44 - 0.0168J(\text{HD})$ (ref 12b). ^b Measured by solid-state NMR (ref 41). Neutron diffraction distances for $\text{Mo}(\text{CO})(\text{dppe})_2$ are about 0.07 Å lower because H_2 rotation foreshortens the $\text{H}-\text{H}$ bond (ref 4). ^c In equilibrium with dihydride tautomer in solution.

$(\text{CO})(\text{H}_2)(\text{dppe})_2$ (0.5–0.6 kcal/mol).^{4a} In addition to the degree of back-bonding present, the barrier is strongly influenced by distortions of the MP_4 skeleton in diphosphine complexes, as has been demonstrated by calculations by Eisenstein.^{4a} The barrier would essentially be zero if the ligands cis to H_2 were perfectly 4-fold symmetric. However, as distortions of the phosphines away from octahedral positions increase, so do the barriers to H_2 rotation, which depend on differences in back-bonding between H_2 orientations. From electronic arguments alone, the decreased back-donation in the Mn cation should have given a lower barrier than that for the Mo complex. However, the Mn complexes are also structurally less distorted than the Mo analogues, so it appears that the higher barriers observed for the cationic complexes could be a result of other factors, perhaps influence by the anion. Rotational barriers have indeed been shown to be very sensitive to the environment near the H_2 , including even variations in lattice solvent.^{4a} The similarity of the barrier for the Mn–dppe and –depe complexes thus could be a result of steric influences rather than electronic considerations, but it is nonetheless consistent with the low influence of the cis ligands on the properties of H_2 binding here.

Assessment of the Activation of Dihydrogen in $[\text{Mn}(\text{CO})(\text{diphosphine})_2(\text{H}_2)]^+$ and Related Complexes: Trans Ligand Effects Dominate. Molecular H_2 coordination chemistry affords a grand opportunity to study how metals activate and oxidatively add H_2 as a function of metal–ligand sets and overall charge of the complex. Conversely, H_2 coordination can be used to probe site-specific electronics on a wide variety of metal fragments. When the $\text{H}-\text{H}$ bond lengths and $J(\text{HD})$ NMR couplings for series of neutral, cationic, and dicationic group 6–8 H_2 complexes with trans-CO ligands are compared (Table 10), a surprising consistency is observed despite the large variation in electrophilicity of the metal. Because $\text{M}-\text{H}_2$

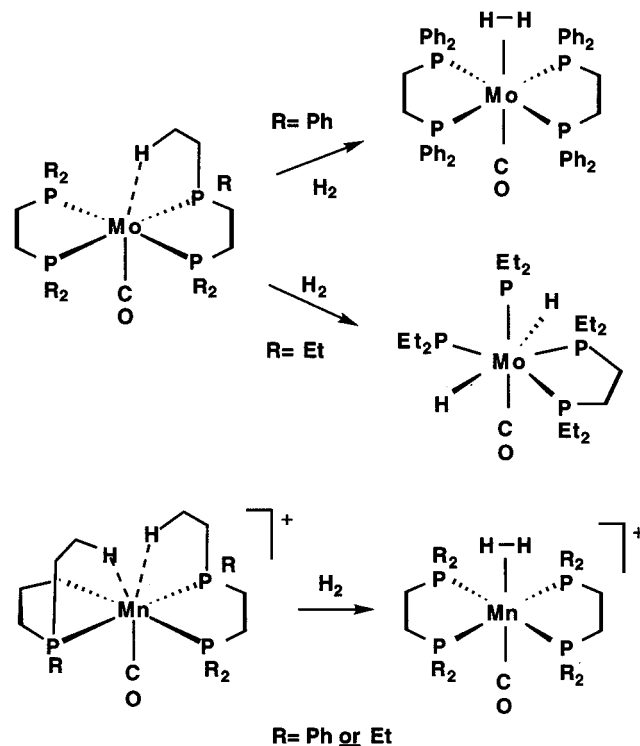
W. T.; Koetzle, T. F.; Fortin, J. B.; Ricci, J. S.; Eckert, J.; Fong, T. P.; Lough, A. J.; Morris, R. H.; Golombek, A. P. *Inorg. Chim. Acta* **1997**, 259, 351. (f) Eckert, J.; Blank, H.; Bautista, M. T.; Morris, R. H. *Inorg. Chem.* **1990**, 29, 747.

bonding is governed by both the Lewis acid strength of the metal for σ bonding (donation from H_2) and the π back-bonding ability of the metal (H_2 as an acceptor), the observed H–H bond length results from a balance of these two bonding components. Thus, the activation of coordinated H_2 in the electropositive systems is occurring primarily via increased σ donation from H_2 as compared to the electron-rich neutral systems where back-donation dominates. As stated in the Introduction, theoretical studies^{1,2} indicate that E_{BD} is about twice as strong as E_D in $Mo(CO)(PH_3)_4(H_2)$, but this is reversed for electron-poor $Mo(CO)_5(H_2)$.^{1b} The nature of the metal is of minor importance compared to the effects of changing the ligand set or charge. Importantly, the sum of the bonding energies of the two components remains nearly constant in a particular system such as $M(CO)_n(PH_3)_{5-n}(H_2)$, and for highly electrophilic metal centers, the loss in back-bonding is almost completely offset by increased σ donation from H_2 to the electron-poor metal center. The extremely electron-poor dication $[Fe(CO)(dppe)_2(H_2)]^{2+}$ actually binds H_2 more strongly than the neutral complexes that are stabilized by back-bonding (unlike the Mn^+ and Mo^0 analogues, the Fe^{2+} complex is stable *in vacuo*^{5a}). Although theoretical calculations for such cationic H_2 systems have not yet been reported, preliminary *ab initio* results for $[Mn(CO)(diphosphine)_2(H_2)]^+$ versus the neutral Mo analogue indicate this to be true.^{3c} Computations²⁵ for CO coordination in $[M(CO)_6]^n$ (M = group 4–9 metal; n = –2 to +3) show that σ donation from CO increases as positive charge increases, just as for H_2 . The first CO dissociation energy is in fact *higher* for the cationic $[M(CO)_6]^n$ complexes, which clearly would not have been expected on the basis of back-bonding arguments alone.^{25b}

The consistency in H–H activation on both the cationic and neutral fragments is nonetheless astonishing, especially in terms of $J(HD)$ values which occur in the narrow range of 32–34 Hz for 19 of the 23 complexes listed in Table 10. This suggests a limit to the activation of the H–H bond by complexes that bind H_2 principally through the σ interaction. This should be expected since the 3-center 2e interaction of a vacant d orbital with the filled H_2 σ orbital limits depletion of the electron density between the two hydrogen atoms as compared to population of the H_2 σ^* orbital, which ultimately can lead to total rupture of the H–H bond. Most of the H–H bond lengths for the cationic systems lie in the relatively narrow range of 0.86–0.90 Å, similar to the calculated distance in $triangulo H_3^+$, 0.87 Å,²⁶ a good model for H_2 activation strictly through σ interactions only. Stable d^0 $M-H_2$ complexes have not been isolated because back-donation cannot take place here. However, cationic H_2 complexes still must retain some degree of back-bonding because they are isolatable and the CO stretching frequencies for $[Mn(CO)(diphosphine)_2(H_2)]^+$ are significantly higher than those for the corresponding agostic complexes. The H–H bond is a much stronger π acceptor compared to the C–H bond in agostic interactions and metal–alkane complexes because orbital mismatch for $M(\eta^2-CH)$ greatly diminishes back-donation.²⁷ According to Ziegler's calculations,^{1b} a moderate amount of back-bonding to H_2 is present even in $Mo(CO)_5(H_2)$, indicating that H_2 competes well with CO for back-bonding. Experimental evidence for the latter is the fact that $\nu(CO)$ undergoes almost

no change when the H_2 ligand in $[Mn(CO)(depe)_2(H_2)]^+$ is replaced by CO (1887 versus 1888 cm^{-1}).

Significantly, H_2 binds molecularly to $Mo(CO)(dppe)_2$ but undergoes oxidative addition on more electron-rich $Mo(CO)(depe)_2$ (and also on $W(CO)(dppe)_2$ ²⁸ because of the increased back-bonding ability of W over Mo).^{4a} However, for the cationic Mn species, H_2 binds molecularly to both the dppe and depe congeners. The positive charge disfavors H–H bond rupture



compared to the neutral systems. Surprisingly, $J(HD)$ is slightly lower, and the H–H bond distance is slightly longer in $[Mn(H_2)(CO)(dppe)_2]^+$ than in the depe analogue. This same counterintuitive pattern has also been seen in the group 8 $[Ru(H_2)(H_2)(PP)_2]^+$ system where $J(HD)$ is 32 Hz when PP is either dppe or depe, despite electrochemical properties and the pK_a of η^2-H_2 showing increased electron richness at the metal for depe.²⁹ On the other hand, in the series $[Re(H_2)(CO)_n\{P(OEt)_3\}_{5-n}]^+$, $J(HD)$ decreases from 33 to 30 Hz as n increases from one to three (increasing electrophilicity), which is an even more emphatic reversal of the expected trend. A few other cationic systems show little variation in H–H activation with changes in relative donor/acceptor ability of the cis-ligand sets, and it has been previously noted that “unstretched” H_2 complexes (H–H < 0.9 Å) do not show very large changes in $J(HD)$ on ligand variation.^{13c} It is thus now quite clear that the nature of the cis ligands has little systematic effect in these cations, especially when compared to neutral complexes at the brink of oxidative addition such as $Mo(CO)(H_2)(PP)_2$. The H–H bond in the latter system is so close to cleaving (the lowest $J(HD)$ observed for any complex with trans CO is 30 Hz for PP = dBzpe) that cis-ligand variation does give a predictable, meaningful trend.

(25) (a) Ehlers, A. W.; Ruiz-Morales, Y.; Baerends, E. J.; Ziegler, T. *Inorg. Chem.* **1997**, *36*, 5031. (b) Szilagyi, R. K.; Frenking, G. *Organometallics* **1997**, *16*, 4807.

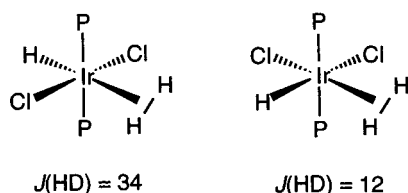
(26) (a) Pang T. *Chem. Phys. Lett.* **1994**, *228*, 555. (b) Farizon, M.; Farizon-Mazuy, B.; de Castro Faria, N. V.; Chermette, H. *Chem. Phys. Lett.* **1991**, *177*, 451.

(27) Saillard, J.-Y.; Hoffmann, R. *J. Am. Chem. Soc.* **1984**, *106*, 2006.

(28) Ishida, T.; Mizobe, Y.; Hidai, M. *Chem. Lett.* **1989**, *11*, 2077.

(29) (a) Bautista, M. T.; Cappellani, E. P.; Drouin, S. D.; Morris, R. H.; Schweitzer, C. T.; Sella, A.; Zubkowski, J. *J. Am. Chem. Soc.* **1991**, *113*, 4876. (b) Cappellani, E. P.; Drouin, S. D.; Jia, G.; Maltby, P. A.; Morris, R. H.; Schweitzer, C. T. *J. Am. Chem. Soc.* **1994**, *116*, 3375.

Despite the tradeoff in σ donation and π back-donation in $M-H_2$ bonding, some structure-bonding aspects of H_2 coordination remain unaccountable. The theoretical model for $Mo(CO)(dppe)_2(H_2)$ features high back-bonding, yet the actual complex has one of the highest $J(HD)$ values and shortest $H-H$ distances known. This is even more puzzling when compared to the cationic Mn congeners that actually have somewhat lower $J(HD)$, longer $H-H$ distances, and no proclivity to cleave the H_2 on increasing the donor strength of the cis-phosphines. Other types of H_2 complexes with different ligand sets, including cationic species such as $[OsH(H_2)(PP)_2]^+$,²⁹ show much lower $J(HD)$ in the 11–26 Hz range. The obvious explanation is that the nature of the ligand trans to H_2 , which is the strong π -acceptor CO for all complexes in Tables 8 and 10, has a powerful leveling effect that may be underestimated in theoretical analyses. The trans effect is of critical importance^{2d,30} in H_2 binding as in all of coordination chemistry, and indeed a comprehensive survey (Table 10) shows that $J(HD) < 30$ Hz is unknown for η^2 -HD trans to CO. As a corollary, $H-H$ distances rarely are observed to be much longer than 0.9 Å in complexes with CO trans to H_2 , regardless of ligand set or overall charge. However, complexes with mild σ -donor ligands trans to H_2 or π -donors such as chloride have greatly elongated $H-H$ bonds (0.96–1.34 Å) and $J(HD)$ from 9 to 28 Hz because of increased back-bonding to H_2 . A good comparison is between the second-row group 6 and 7 congeners, $Mo(CO)(H_2)(dppe)_2$ ($J(HD) = 34$ Hz; $H-H = 0.88$ Å) and $TcCl(H_2)(dppe)_2$ where $H-H$ elongates 0.2 Å to 1.08 Å.³¹ $[RuCl(H_2)(dppe)_2]^+$ has a $J(HD)$ of 26 Hz, much lower than that for congeners with trans CO or hydride,³² and analogues with alkyl diphosphines have an even lower value of 16 Hz, showing strong, unmitigated H_2 activation. If the trans ligand is a strong σ -donor such as hydride, there is a potent trans labilizing effect that reduces σ donation from H_2 , which once again weakens $M-H_2$ binding strength and contracts the $H-H$ distance ($J(HD)$ generally > 28 Hz). Certain electron-rich neutral complexes with hydride trans to H_2 such as *trans*- $IrCl_2H(H_2)(PR_3)_2$ ^{30b} actually bind H_2 more weakly than many of the highly electrophilic cationic systems.



For *cis*- $IrCl_2H(H_2)(PR_3)_2$, $J(HD)$ decreases dramatically to 12 Hz and ab initio calculations ($R = H$) show a spectacular increase in $H-H$ distance from 0.81 to 1.4 Å (1.11 Å experimental for $R = i\text{-Pr}$) on going from the trans to the cis isomer.^{30b} Although the hydride cis to H_2 in the latter has some influence (cis effect), the influence of the trans ligand on H_2 activation generally far exceeds that of the entire cis-ligand set. This is true particularly in cations with trans CO where back-bonding effects are lower. This enormous dependence on fragment stereochemistry can be expected to extend to other σ complexes, including alkane complexes where back-donation to $C-H$ is much lower.

Comparative Binding of Other Ligands to $[Mn(CO)(dppe)_2]^+$. In regard to silane coordination on group 6 systems,³³ $[Mn(CO)(dppe)_2][BAr'_4]$ binds SiH_4 much more weakly than $Mo(CO)(depe)_2$, which gives a tautomeric equilibrium between the σ complex and the oxidative addition product.^{33a} A $Mn-SiH_4$ complex could not even be observed, because the H_2 always present as an impurity in SiH_4 coordinated more strongly. Organosilanes also did not give stable complexes, even at -70 °C. Coordination of silanes to first row group 6 and 7 metals thus appears to be much weaker than to second and third row metals as $PhSiH_3$ did not bind at all to $M(CO)_3(PR_3)_2$ for Cr and Mn^+ but underwent oxidative addition for W.^{3d,33c} This may be a result of increased steric congestion at the smaller first row metal when bulky phosphines are present. In general, silane binding and activation is much more variable with respect to the metal fragment than that for H_2 , which coordinates in a much more steady fashion throughout first to third row metals and, for the most part, oxidatively adds more predictably.^{33c}

Poor bases such as Et_2O and CH_2Cl_2 do not bind to the Mn -diphos complexes, indicating that they are not as electrophilic as $[Re(CO)_4(PCy_3)]^+$ and $[PtH(PPr'_i)_2]^+$, which do.^{3b,c} Surprisingly, the normally strong amphoteric ligand SO_2 , which irreversibly binds to the neutral Mo analogues and most transition-metal fragments,^{14a} coordinates weakly and reversibly to $[Mn(CO)(dppe)_2]^+$, as found for $[Mn(CO)_3(PCy_3)_2]^+$.^{3d} As recently concluded, there is a clear trend that electrophilic cationic systems favor H_2 binding over N_2 and even stronger π acceptors such as SO_2 .^{3d} Although H_2 is generally considered to be a "weak" ligand, the highly amphoteric nature of H_2 bonding to transition metals makes H_2 much more versatile than N_2 , olefins, silanes, and virtually any other ligand. Dihydrogen is thus able to stably coordinate or oxidatively add to a wider array of transition-metal fragments (except d^0 systems, which cannot back-donate), particularly cationic species, than even most "strong" ligands.

Conclusions

The electrophilic 16e $[Mn(CO)(PP)_2]^+$ complexes ($PP =$ diphosphine) are stabilized by low-coordinating boron or gallium anions and contain weak polyagostic interactions reversibly displaceable by H_2 and N_2 . The large new gallium anion $[(Ga(C_6F_5)_3)_2(\mu-Cl)]^-$ is reported, which along with $[Ga(C_6F_5)_4]^-$ is a useful counterion for neutron scattering studies. The $Mn \cdots H-C$ distances are much longer than those found for the single interactions in $Mo(CO)(PP)_2$ and $[Mn(CO)_3(PCy_3)_2]^+$ and are more characteristic of van der Waals contacts, especially for the depe complex. The $H-H$ and also the $Mn-H$ distances have been determined in $[Mn(H_2)(CO)(dppe)_2]^+$ in solution by NMR T_1 measurements on both the H_2 and HD isotopomers. This method is potentially useful for other H_2 complexes, especially for metal centers with high nuclear spin. IR data and $C-O$ and $M-C$ bond lengths are used to gauge the π -acceptor strengths of ligands trans to the CO. The agostic $C-H$ bonds are the weakest "ligands" and also the weakest acceptors, with $\nu(CO)$ similar to that for pure σ donors such as NH_3 . In contrast, H_2 , N_2 , and ethylene are excellent acceptors. The $C-O$ bond length always decreases, and the $M-C$ bond length increases when these acceptor ligands replace the agostic interactions. The variation of $\nu(CO)$ on increasing the basicity of the cis-

- (30) (a) Schlaf, M.; Lough, A. J.; Maltby, P. A.; Morris, R. H. *Organometallics* **1996**, *15*, 2270, and references therein. (b) Albinati, A.; Bakmutov, V. I.; Caulton, K. G.; Clot, E.; Eckert, J.; Eisenstein, O.; Gusev, D. G.; Grushin, V. V.; Hauger, B. E.; Klooster, W. T.; Koetzle, T. F.; McMullan, R. K.; O'Loughlin, T. J.; Pelissier, M.; Ricci, J. S.; Sigalas, M. P.; Vymenits, A. B. *J. Am. Chem. Soc.* **1993**, *115*, 7300.
- (31) Burrell, A. K.; Bryan, J. C.; Kubas, G. J. *J. Am. Chem. Soc.* **1994**, *116*, 1575.
- (32) Chin, B.; Lough, A. J.; Morris, R. H.; Schweitzer, C.; D'Agostino, C. *Inorg. Chem.* **1994**, *33*, 6278.

- (33) (a) Luo, X.-L.; Kubas, G. J.; Burns, C. J.; Bryan, J. C.; Unkefer, C. J. *J. Am. Chem. Soc.* **1995**, *117*, 1159. (b) Luo, X.-L.; Kubas, G. J.; Bryan, J. C.; Burns, C. J.; Unkefer, C. J. *J. Am. Chem. Soc.* **1994**, *116*, 10312. (c) Butts, M. D.; Kubas, G. J.; Luo, X.-L.; Bryan, J. C. *Inorg. Chem.* **1997**, *36*, 3341.

phosphines in *trans*-M(CO)(PP)₂(L) for L = H₂ and N₂ is far less than that for increasing charge (M = Mn⁺ vs Mo).

There is a fine balance between H₂ → M donation and M → H₂ back-donation in the activation of the H–H bond. In highly electrophilic cationic systems, increased σ donation compensates for the reduction of back-bonding prevalent in more electron-rich neutral analogues. Thus, the H–H bond lengths and *J*(HD) of [Mn(CO)(PP)₂(H₂)]⁺ and other cationic complexes with H₂ trans to CO are strikingly similar to their neutral analogues and nearly invariant. The ligand trans to H₂ controls the H–H distance more so than all of the cis ligands combined and placement of a *strong acceptor such as CO trans to an open coordination site in a cationic group 5–10 system virtually guarantees formation of a M(η²-X–H) σ complex regardless of the metal or cis ligands.* This would not have been expected from the accepted principle that increased electron richness at the metal lengthens the H–H bond, and thus the viewpoints on M–H₂ bonding and activation continue to evolve. In this context, hydrogenase enzymes that catalyze interconversion of H₂ and protons contain strong π-acceptor ligands such as CO and CN rarely seen in biological systems.³⁴ The molecular binding and activation of H₂ could thus be elegantly controlled at the binding site merely by cis versus trans disposition of the acceptor ligands.

Experimental Section

MnBr(CO)₅, GaCl₃, C₆F₅Br, and Li(*n*-butyl) were purchased from Aldrich Chemical Co., and depe from Strem Chemical Co. MnBr(CO)(dpepe)₂^{3a} and Na[BAR'₄]^{10b} were prepared according to literature methods. C₆H₆ was distilled from Na/K alloy and hexane, and Et₂O from Na/benzophenone under Ar. UHP grade gases were used for all procedures. CO and SO₂ were purchased from Matheson and used without further purification. Solids were manipulated in a Vacuum Atmospheres drybox under a He atmosphere. Hexane used for LiGa(C₆F₅)₄ preparation was scrubbed of olefins with H₂SO₄ and then distilled under Ar from Na/K alloy. CH₂Cl₂ was distilled from P₂O₅ or CaCl₂. MnBr(CO)(depe)₂, LiGa(C₆F₅)₄, and Li[Ga(C₆F₅)₄·2Et₂O] were prepared using standard Schlenk techniques. Cationic metal complexes were prepared using standard high vacuum techniques in CH₂Cl₂ and C₆H₅F solvents freshly vacuum transferred from P₂O₅ or CaH₂. Hexanes used in preparing cationic systems were vacuum transferred from Na/K alloy. NMR measurements were performed on Bruker WM300 MHz, Varian Unity 300 MHz, and Bruker AMX500 MHz instruments. FTIR measurements were performed on a Biorad FTIR Spectrometer.

Synthesis of MnBr(CO)(depe)₂. MnBr(CO)₅ (1.432 g, 5.209 mmol) and depe (2.617 g, 12.69 mmol) were added to 200 mL of benzene. The orange reaction mixture was irradiated for 3 h under a N₂ or Ar flush with a medium-pressure Hg lamp using a quartz water-jacketed immersion well. On completion, the yellow solution was filtered under Ar. The volume of the benzene was reduced, and the product was precipitated with hexane, isolated by filtration, and dried in vacuo (yield, 55%). Further purification can be afforded by precipitation from toluene with anhydrous ethanol. Anal. Calcd for C₂₁H₄₈BrOP₄Mn: C, 43.8%; H, 8.41%. Found: C, 43.8%; H, 8.50%. ¹H NMR (CD₂Cl₂): δ 2.3–1.1 (m, 48H, depe). ³¹P{¹H} NMR (121.42 MHz, CD₂Cl₂): δ 74.2. IR (Nujol mull): ν(CO) 1803 cm⁻¹.

Synthesis of Li[Ga(C₆F₅)₄]. GaCl₃ was sublimed, and C₆F₅Br was dried over P₂O₅ and vacuum transferred prior to use. Trace olefins were removed from hexane by treatment with H₂SO₄ and distillation from Na/K alloy (a critical step in the synthesis). Under an Ar atmosphere, C₆F₅Br (32.03 g, 0.1297 mol) was added to 500 mL of hexane and cooled to –78 °C. The reaction mixture was then charged with 52 mL of 2.5 M *n*-BuLi. A white precipitate formed on addition. GaCl₃ (5.70 g, 0.0324 mol) was dissolved in 100 mL of hexane. The GaCl₃ was

added slowly to the LiC₆F₅ over 30 min. The reaction was allowed to slowly warm over a period of 16 h to room temperature. The hexane was filtered off the solids, which were then extracted with 250 mL of toluene. The extraction was repeated with 200 mL of toluene, all of which was then removed in vacuo. The solids were taken up in 75 mL of CH₂Cl₂ and then precipitated with 120 mL of hexane. The volume was reduced 75%, and then 90 mL of hexane was added to complete the precipitation. The solution was filtered off, and the product was dried in vacuo. Yield: 6.033 g. A second extraction was performed on the reaction residues yielding 4.500 g of product. Overall yield: 44%. The reaction product gave a positive Li flame test and a negative AgCl test. Although the product did not give consistent elemental analysis, ¹⁹F and ¹³C NMR spectroscopy in THF-*d*₈ of the anion was consistent with that previously reported for [Bu₄N][Ga(C₆F₅)₄].⁸ The product was found by ¹⁹F NMR to contain minor amounts of impurities that did not affect its further use. ¹³C (THF-*d*₈): δ 150.0 (*J*_{C–F} = 237.8 Hz, ortho); 140.8 (*J*_{CF} = 249.2 Hz, meta); 137.3 (*J*_{CF} = 236.5, para); 121.5. ¹⁹F (THF-*d*₈): –123.1 (d, 8F, ortho), –160.5 (t, 4F, para), –165.4 (t, 8F, meta).

Synthesis of Li[Ga(C₆F₅)₄·2Et₂O. C₆F₅Br was dried over P₂O₅ and vacuum transferred prior to use. Under an Ar atmosphere, C₆F₅Br was dissolved in 150 mL of Et₂O and cooled to –78 °C. The reaction mixture was then charged with 4.2 mL of 1.6 M *n*-BuLi and allowed to stir for 10 min. Ga(C₆F₅)₃·Et₂O in 100 mL of Et₂O was added to the solution, and then the reaction was allowed to warm to room temperature and stirred over 20 h. The volume of the solution was reduced in vacuo 75%. The solution was filtered and then cooled to –78 °C. The colorless precipitate was filtered off and stirred with hot hexane, forming an oil that solidified on cooling. The hexane was decanted off the solids, which were dried in vacuo. The product gave a positive flame test for Li. Anal. Calcd for C₃₂H₂₀F₂₀GaLi₄O₂: Ga, 7.83%. Found: Ga, 7.77%. ¹H NMR (THF-*d*₈): 3.36 (q, 4H, CH₂); 1.10 (t, 6H, CH₃). ¹³C (THF-*d*₈): 149.8 (*J*_{CF} = 232.2 Hz, ortho); 140.8 (*J*_{CF} = 249.8 Hz, meta); 137.2 (*J*_{CF} = 271.5 Hz, para); 121.5. ¹⁹F (C₆D₆ (1 mL) + THF (0.3 mL)): –123.0 (d, 8F, ortho); –159.3 (t, 4F, para); –164.6 (t, 8F, meta).

In Situ Generation of [Mn(CO)(depe)₂][BAR'₄]. A J. Young NMR tube was charged with MnBr(CO)(depe)₂ (0.011 g, 0.019 mmol) and Na[BAR'₄] (0.017 g, 0.019 mmol) in a He-filled Vacuum Atmospheres drybox. The NMR tube was quickly charged with C₆D₅F and closed off. On shaking, a deep blue solution was formed. The yield of [Mn(CO)(depe)₂]⁺ was essentially quantitative by ³¹P NMR. ¹H NMR (C₆D₅F): δ 8.32 (s, 8 H, C₆H₃(CF₃)₂, ortho); 7.65 (s, 4 H, C₆H₃(CF₃)₂, para); 1.6–0.9 (m, 48H, depe). ³¹P{¹H} NMR (C₆D₅F): δ 81.4 (s).

Large-Scale Synthesis of [Mn(CO)(depe)₂][BAR'₄]. The reaction was run under conditions identical to those for [Mn(CO)(depe)₂(H₂)]-[BAR'₄] below but under an atmosphere of Ar. On completion of the reaction, a deep blue solution had formed. During filtration and vacuum transfer of the hexane onto the reaction solution, a slight yellowing of the reaction mixture was detected. From 0.515 g (0.895 mmol) of MnBr(CO)(depe)₂ and 0.918 g (1.03 mmol) of Na[BAR'₄], 1.180 g of product was isolated. NMR revealed that the product contained a mixture of [Mn(CO)(depe)₂]⁺ and [Mn(CO)₂(depe)₂]⁺ cations by ³¹P NMR. Integration of the respective ³¹P NMR signals showed the presence of 15% [Mn(CO)₂(depe)₂][BAR'₄]. The latter was identified by reacting an in situ generated sample of [Mn(CO)(depe)₂]⁺ with CO (see below). The dicarbonyl complex presumably resulted from minor decomposition of the agostic complex by trace O₂ during filtration and vacuum transfer steps.

In Situ Generation of [Mn(CO)(depe)₂][Ga(C₆F₅)₄]. A J. Young NMR tube was charged with MnBr(CO)(depe)₂ (0.019 g, 0.01 mmol) and Li[Ga(C₆F₅)₄] (0.030 g, 0.040 mmol) in a He-filled Vacuum Atmospheres drybox. The NMR tube was quickly charged with C₆D₅F and closed off. On shaking, a deep blue solution was formed. The yield of the cation was quantitative by ³¹P NMR. ¹H NMR (C₆D₅F): δ 1.8–0.7 (m, 48H, depe). ³¹P{¹H} NMR (121.42 MHz, C₆D₅F): δ 80.3 (s).

Synthesis of [Mn(CO)(depe)₂(H₂)]-[BAR'₄]. Fluorobenzene (10–15 mL) was vacuum transferred onto MnBr(CO)(depe)₂ (0.551 g, 0.957 mmol) and Na[BAR'₄] (0.902 g, 1.02 mmol) at –78 °C. The reaction was then placed under a positive pressure of H₂ and allowed to warm to room temperature. As the solution thawed and the reaction began stirring, the color changed from yellow to blue green. After reaction

(34) See, for example: Pavlov, M.; Siegbahn, P. E. M.; Blomberg, M. R. A.; Crabtree, R. H. *J. Am. Chem. Soc.* **1998**, *120*, 848, and references therein.

with H₂ over the solution, the color became light yellow. After 45 min, the solution was filtered, and volume was reduced by half. On reduction in volume, the solution became green, but on backfilling with H₂, the solution became yellow again. The solution was cooled to -78 °C, and then hexane was vacuum transferred onto the frozen yellow fluorobenzene solution. Care must be taken to not vacuum transfer hexane onto the blue agostic intermediate, as trace amounts of O₂ present in the system will react with it. The product mixture was placed under H₂ and allowed to warm to room temperature. On warming and mixing of the solvents, a light yellow precipitate formed. The product was isolated by filtration and dried in vacuo for 1 h. During this time, the solid became light blue as H₂ was released. The solid was then placed under H₂, and the resulting yellow solid was isolated and stored under H₂. Yield: 87.3%. ¹H NMR (C₆D₆F): δ 8.31 (s, 8 H, C₆H₃-(CF₃)₂, ortho); 7.63 (s, 4 H, C₆H₃(CF₃)₂, para); 1.7–0.7 (m, 48H, depe); -10.25 (s, 19 Hz fwhm at 500 MHz, 2H, Mn–H₂). ³¹P{¹H} NMR (C₆D₆F): δ 83.5 (s). IR (Nujol mull): ν(CO) 1896 cm⁻¹.

Synthesis of [Mn(CO)(depe)₂(N₂)][BAR'4]. The complex was prepared under identical conditions to the above H₂ complex but under an atmosphere of N₂ using MnBr(CO)(depe)₂ (0.411 g, 0.714 mmol) and Na[BAR'4] (0.902 g, 1.02 mmol). The complex was produced in 86% yield and was stored under N₂. The bound N₂ possesses a similar lability to that of bound H₂. ¹H NMR (C₆D₆F): δ 8.32 (s, 8H, C₆H₃-(CF₃)₂, ortho), 7.64 (s, 4 C₆H₃(CF₃)₂, para); δ 1.7–0.9 (m, 48 H, depe). IR (Nujol mull, cm⁻¹): ν(CO), 1896; ν(NN), 2146.

Synthesis of [Mn(CO)(depe)₂(H₂)] [Ga(C₆F₅)₄]. The compound was prepared under identical conditions to [Mn(CO)(depe)₂(H₂)] [BAR'4] from MnBr(CO)(depe)₂ (2.010, 2.094 mmol) and Li[Ga(C₆F₅)₄] (2.507 g, 3.366 mmol) in 84% yield. ¹H NMR (C₆D₅F): δ 1.7–0.8 (m, 48H, depe), -10.23 (s, 25 Hz fwhm at 500 MHz, 2H, Mn–H₂). ³¹P{¹H} NMR (C₆D₅F): δ 83.4 (s).

Synthesis of [Mn(CO)(depe)₂(D₂)] [Ga(C₆F₅)₄]. The compound was prepared under conditions identical to the above with the exception that the reaction was run under D₂. Using MnBr(CO)(depe)₂ (1.508, 1.571 mmol) and Li[Ga(C₆F₅)₄] (1.898 g, 2.548 mmol), the complex was produced in 84% yield. ¹H NMR (C₆D₅F): δ 1.5–0.6 (m, 48H, depe). ³¹P{¹H} NMR (C₆D₅F): δ 83.3 (s).

Synthesis of [Mn(CO)(dppe)₂] [Ga(C₆F₅)₄]. Toluene (30 mL) was vacuum transferred onto MnBr(CO)(dppe)₂ (2.012 g, 2.096 mmol) and Li[Ga(C₆F₅)₄] (2.855 g, 3.833 mmol) at -78 °C. The reaction was warmed to room temperature and stirred for 30 min, yielding a blue solution. The toluene was removed in vacuo, and the residue was extracted with CH₂Cl₂. The blue solution was filtered, and the product was crystallized by reduction of volume of the CH₂Cl₂ and addition of hexane by vacuum transfer at -20 to -30 °C. A blue oil formed and then solidified. The resulting light blue supernatant was decanted off, and the product was dried in vacuo for 3 h. Yield: 96%. ¹H NMR (CD₂Cl₂): δ 7.3–7.1 (m, 24 H, C₆H₅); 6.23 (m, 16 H, C₆H₅); 2.79 (m, 8 H, PCH₂CH₂P). ³¹P{¹H} NMR (CD₂Cl₂): δ 83.0 (s).

Synthesis of [Mn(CO)(dppe)₂(H₂)] [Ga(C₆F₅)₄]. Method A. The compound was prepared under conditions identical to those for [Mn(CO)(depe)₂(H₂)] [BAR'4] with the following modifications. CH₂Cl₂ was used as the reaction solvent, and MnBr(CO)(dppe)₂ (0.958, 0.998 mmol) and Li[Ga(C₆F₅)₄] (1.195 g, 1.604 mmol) were the reactants. The final product was crystallized from a mixture of 5 mL of CH₂Cl₂ and 50 mL of hexane (yield: 1.721 g). ³¹P NMR was found to be clean, but the product contains a slight amount of unreacted Li[Ga(C₆F₅)₄] which was present in excess. ¹H NMR (CD₂Cl₂): δ 7.4–7.0 (m, 40H, C₆H₅); 2.50 (m, 4H, PCH₂CH₂P); 2.24 (m, 4H, PCH₂CH₂P); -7.22 (s, 2H, 33 Hz fwhm at 300 MHz, Mn–H₂). ³¹P{¹H} NMR (CD₂Cl₂): δ 85.9 (s).

Method B. CH₂Cl₂ (20 mL) was vacuum transferred onto [Mn(CO)(dppe)₂] [Ga(C₆F₅)₄] (2.007 g, 1.240 mmol). The resulting solution was placed under an atmosphere of H₂ and quickly turned from blue to yellow. [Mn(CO)(dppe)₂(H₂)] [Ga(C₆F₅)₄] precipitated out partially from solution and was isolated by reduction of solution volume at -20 to -30 °C and precipitation with hexane. Yield: 95.9%.

Synthesis of [Mn(CO)(dppe)₂(D₂)] [Ga(C₆F₅)₄]. The compound was prepared by Methods A and B above except under an atmosphere of D₂. NMR resonances were identical except for the absence of the signal at δ -7.22 due to Mn–H₂.

In Situ Generation of [Mn(CO)₂(depe)₂] [BAR'4]. A J. Young NMR tube was charged with MnBr(CO)(depe)₂ (0.009 g, 0.01 mmol) and Na[C₆H₃(3,5-CF₃)₂]₄] (0.015 g, 0.017 mmol) in a He-filled Vacuum Atmospheres drybox. The NMR tube was quickly charged with C₆D₅F and closed off. On shaking, a deep blue solution was formed. The NMR tube was attached to a vacuum line and the solvent was cooled to -196 °C. The He atmosphere was removed, and the tube was backfilled with CO, resulting in a light yellow solution. Yield: 100% by ³¹P NMR. ¹H(C₆D₅F): δ 8.63 (s, 8 H, C₆H₃(CF₃)₂, ortho); 7.96 (s, 4 H, C₆H₃-(CF₃)₂, para); δ 1.9–1.2 (m, 48H, depe). ³¹P{¹H} NMR (121.42 MHz, CD₂Cl₂): δ 75.8 (s).

Generation of [Mn(CO)₂(depe)₂] [BAR'4]. A 0.04 g solid sample of material from the large scale synthesis of [Mn(CO)(depe)₂] [BAR'4] was placed under an atmosphere of CO until the blue color of the agostic complex had bleached completely, yielding 0.04 g of light yellow solid. IR: ν(CO) 1888 cm⁻¹.

Competition Study of Binding H₂ and N₂ to [Mn(CO)(depe)₂] [BAR'4] and [Mn(CO)(dppe)₂] [BAR'4]. A typical procedure was performed as follows. A 1-L ballast was evacuated to 5 × 10⁻⁵ mmHg. At 77 K, the ballast was charged to 307.5 mmHg with N₂ and then charged to 615.6 mmHg with H₂. The ballast was allowed to warm until the pressure had risen to 820.0 mmHg. A J. Young NMR tube containing in situ generated [Mn(CO)(depe)₂] [BAR'4] in C₆D₅F cooled to 195 K was evacuated, exposed to the gas from the ballast, and warmed to room temperature. The sample was allowed to equilibrate with the gas mixture on completion of the reaction, as evidenced by the bleaching of the blue color of the agostic complexes. The NMR tube was then closed off, and the solution was analyzed by NMR as described in the Results Section.

Synthesis of Mn(CO)(SO₂)(dppe)₂] [BAR'4]. CH₂Cl₂ (15 mL) was vacuum transferred onto MnBr(CO)(dppe)₂ (0.315 g, 0.328 mmol) and Na[BAR'4] (0.307 g, 0.346 mmol) at -78 °C. The reaction vessel was backfilled with SO₂ and allowed to warm to room temperature under positive pressure of SO₂. The reaction was allowed to stir for 30 min. The solution color initially changed from yellow orange to blue, and as the SO₂ reacted, it became orange. The solution was filtered, and the complex began to lose SO₂, as evidenced by a return of the blue color of agostic complex. The solution was then maintained under an SO₂ atmosphere. Attempts to precipitate the complex from CH₂Cl₂ with 15 mL of hexane, added by vacuum transfer onto the CH₂Cl₂ solution cooled to -78 °C, failed. The CH₂Cl₂ was removed in vacuo, and the resulting oil was stirred with 15 mL of hexane under an atmosphere of SO₂ until the product solidified. The hexane solution was filtered off, and the solid was dried in vacuo. The resulting solid lost SO₂ and was placed under an atmosphere of SO₂ prior to isolation (yield: 0.549 g). The product was stored under SO₂. ¹H NMR (CD₂Cl₂): δ 7.74 (s, 8 H, C₆H₃(CF₃)₂, ortho); 7.52 (s, 4 H, C₆H₃(CF₃)₂, para); 7.48–6.82 (m, 40H, Ph); 3.12 (m, 4H, PCH₂CH₂P); 2.66 (m, 4H, PCH₂CH₂P). ³¹P{¹H} (CD₂Cl₂): δ 67.63.

X-ray Structure Determination of [Mn(CO)(depe)₂] [Ga(C₆F₅)₄]. Crystallographic data are summarized in Table 11. A blue rectangular block was mounted in a capillary and flame sealed. The capillary was then placed on a Bruker P4/CCD/PC diffractometer and cooled to 210 K using a Bruker LT-2 temperature device. The data were collected using a sealed, graphite monochromatized Mo Kα X-ray source. The lattice was determined using 44 reflections. A hemisphere of data was collected using a combination of φ and ω scans, with 30 s frame exposures and 0.3° frame widths. Data collection, initial indexing, and cell refinement were handled using SMART software, and frame integration and final cell parameter calculation were carried out using SAINT software.³⁵ The final cell parameters were determined using a least-squares fit to 2354 reflections. The data were corrected for absorption using SADABS program.³⁶ Decay of reflection intensity was not observed.

(35) (a) SMART Version 4.210, 1996, Bruker Analytical X-ray Systems, Inc., 6300 Enterprise Lane, Madison, Wisconsin 53719. (b) SAINT Version 4.05, 1996, Bruker Analytical X-ray Systems, Inc., Madison, Wisconsin 53719.

(36) SADABS, first release, G. M. Sheldrick, University of Gottingen, Germany.

Table 11. Summary of Crystallographic Data

	[Mn(CO)(depe) ₂] ⁺ [Ga(C ₆ F ₅) ₄] ⁻	[Mn(CO)(depe) ₂ (H ₂) ⁺ [Ga(C ₆ F ₅) ₄] ⁻	[Mn(CO)(dppe) ₂ (H ₂) ⁺ [Cl{Ga(C ₆ F ₅) ₃ } ₂] ⁻
formula	C ₄₅ H ₄₈ OP ₄ F ₂₀ GaMn	C ₄₅ H ₅₀ OP ₄ F ₂₀ GaMn	C ₈₆ H ₅₀ OP ₄ ClF ₃₀ Ga ₂ Mn
fw	1233.37	1235.38	2059.00
T, °C	-163	-76	-135
λ, Å	0.71073	0.71073	0.71073
crystal system	orthorhombic	triclinic	monoclinic
space group	P2 ₁ 2 ₁ 2	P1	C2/c
color	blue	yellow	yellow
a, Å	17.528(4)	12.987(2)	10.224(4)
b, Å	18.192(4)	14.942(2)	32.73(3)
c, Å	8.169(2)	15.622(2)	24.310(9)
α, deg		105.184(6)	90
β, deg		109.207(8)	97.69(3)
γ, deg		103.632(7)	90
ρ _{calcd} , g cm ⁻³	1.573	1.585	1.696
V, Å ³	2604.8(10)	2584.8(6)	8062(8)
Z	2	2	4
μ, mm ⁻¹	0.988		1.050
R [I > 2σ(I)] ^a	0.0738	0.0522	0.0798
R _w [I > 2σ(I)] ^b	0.1442 ^c	0.1462 ^d	0.1884 ^e

^a $R = \sum ||F_o| - |F_c|| / \sum |F_o|$. ^b $R_w = [\sum [w(F_o^2 - F_c^2)^2] / \sum [w(F_o^2)^2]]^{1/2}$. ^c $w = 1/[\sigma^2(F_o^2) + (0.0672 * P)^2]$. ^d $w = 1/[\sigma^2(F_o^2) + (0.0947 * P)^2]$. ^e $w = 1/[\sigma^2(F_o^2) + (0.1064 * P)^2 + 46.6639 * P]$.

The structure was solved in space group P2₁2₁2 using Patterson and difference Fourier techniques. The initial solution revealed the manganese, gallium, and phosphorus atom positions. The remaining atomic positions were determined from subsequent Fourier synthesis. All hydrogen atom positions were fixed using the HFIX command in SHELXTL PC.³⁷ The C–H distances were fixed at 0.96 Å for methyl and 0.97 Å for methylene. The hydrogen atoms were refined using a riding model with their isotropic temperature factors set to 1.5 (methyl) or 1.2 (methylene) times the equivalent isotropic U of the carbon atom they were bound to. Attempts to locate the agostic hydrogen atom positions were not successful. The final refinement included anisotropic temperature factors on all non-hydrogen atoms. Structure solution and graphics were performed using SHELXTL PC. SHELXL-93 was used for structure refinement and creation of publication tables.³⁸

X-ray Structure Determination of [Mn(CO)(depe)₂(H₂)] [Ga(C₆F₅)₄]. Crystallographic data are summarized in Table 11. A yellow rectangular block was mounted in a capillary, flame sealed under H₂, and then placed under a liquid nitrogen cold stream on a Siemens P4/PC diffractometer. The radiation used was graphite monochromatized Mo Kα radiation. The lattice parameters were optimized from a least-squares calculation on 25 carefully centered reflections of high Bragg angle. The data were collected using ω scans with a 0.78° scan range. Three check reflections monitored every 97 reflections showed no systematic variation of intensities. Lattice determination and data collection were carried out using XSCANS Version 2.1b software. All data reduction were performed using SHELXTL PC Version 4.2/360 software. The structure refinement was performed using SHELX-93 software.³⁹

The structure was solved in space group P1̄ using Patterson and difference Fourier techniques. This solution yielded the metal and the

majority of all other atom positions. Subsequent Fourier synthesis gave all remaining non-hydrogen atom positions. The methyl and methylene hydrogen atoms were fixed in positions of ideal geometry, with C–H distances of 0.96 and 0.97 Å, respectively. The hydrogen atoms were refined using the riding model in the HFIX facility in SHELX-93, with their isotropic temperature factors fixed at 1.2 (methylene) or 1.5 (methyl) times the equivalent isotropic U of the carbon atom they were bonded to. Attempts to locate and refine the hydrogen molecule were not successful. The final refinement included anisotropic thermal parameters on all non-hydrogen atoms.

X-ray Structure Determination of [Mn(CO)(dppe)₂(H₂)] [Cl(Ga(C₆F₅)₃)₂]. Crystallographic data are summarized in Table 11. A yellow rectangular plate was mounted on a thin glass fiber using silicone grease. The crystal, which was mounted directly from the reaction vessel under a hydrogen gas flow, was then immediately placed under a liquid nitrogen stream on a Siemens P4/PC diffractometer. The radiation used was graphite monochromatized Mo Kα radiation. The lattice parameters were optimized from least-squares calculation on 25 carefully centered reflections of high Bragg angle. Three check reflections monitored every 97 reflections showed no systematic variation of intensities. Lattice determination and data reduction, including Lorentz polarization corrections and structure solution and graphics, were performed using SHELXTL PC Version 4.2/360 software. The structure refinement was performed using SHELX-93 software.³⁹ The data were not corrected for absorption due to the low absorption coefficient.

Space groups Cc and C2/c were suggested by systematic absences. The structure was initially solved in Cc using direct methods to locate the gallium, chlorine, manganese, and phosphorus atoms. The remaining

(37) SHELXL PC Version 4.2/360, 1994, Bruker Analytical X-ray Systems, Inc., Madison, Wisconsin 53719.

(38) SHELX-93, G. M. Sheldrick, University of Göttingen, Germany.

(39) XSCANS and SHELXTL PC are products of Siemens Analytical X-ray Instruments, Inc., 300 Enterprise Lane, Madison, Wisconsin 53719. SHELX-93 is a program for crystal structure refinement written by G. M. Sheldrick, 1993, University of Göttingen, Germany.

(40) Kubas, G. J.; Nelson, J. E.; Bryan, J. C.; Eckert, J.; Wisniewski, L.; Zilm, K. *Inorg. Chem.* **1994**, *33*, 2954.

(41) Zilm, K. W.; Millar, J. M. *Adv. Magn. Opt. Reson.* **1990**, *15*, 163.

(42) (a) Kubas, G. J.; Ryan, R. R.; Swanson, B. I.; Vergamini, P. J.; Wasserman, H. J. *J. Am. Chem. Soc.* **1984**, *106*, 451. (b) Kubas, G. J.; Unkefer, C. J.; Swanson, B. I.; Fukushima, E. *J. Am. Chem. Soc.* **1986**, *108*, 7000.

(43) Tatsumi, T.; Tominaga, H.; Hidai, M.; Uchida, Y. *J. Organomet. Chem.* **1980**, *199*, 63.

(44) Luo, X.-L.; Michos, D.; Crabtree, R. H. *Organometallics* **1992**, *11*, 237.

(45) Gusev, D. G.; Nietispach, D.; Eremenko, I. L.; Berke, H. *Inorg. Chem.* **1993**, *32*, 3628.

(46) Kubas, G. J.; Burns, C. J.; Khalsa, G. R. K.; Van Der Sluys, L. S.; Kiss, G.; Hoff, C. D. *Organometallics* **1992**, *11*, 3390.

(47) Kubas, G. J.; Ryan, R. R.; Vergamini, P. J., unpublished results.

(48) Van der Sluys, L. S.; Huffman, J. C.; Kubas, G. J., unpublished results.

(49) Bruns, W.; Hausen, H.-D.; Kaim, W.; Schulz, A. *J. Organomet. Chem.* **1993**, *444*, 121.

(50) Lang, R. F.; Ju, T. D.; Kiss, G.; Hoff, C. D.; Bryan, J. C.; Kubas, G. J. *J. Am. Chem. Soc.* **1994**, *116*, 7917.

(51) Kubas, G. J.; Jarvinen, G. D.; Ryan, R. R. *J. Am. Chem. Soc.* **1983**, *105*, 1883.

(52) Andrea, R. R.; Vuurman, M. A.; Stufkens, D. J.; Oskam, A. *Recl. Trav. Chim. Pays-Bas* **1986**, *105*, 372.

(53) Burdett, J. K.; Downs, A. J.; Gaskill, G. P.; Graham, M. A.; Turner, J. J.; Turner, R. F. *Inorg. Chem.* **1978**, *17*, 523.

(54) Albertin, G.; Antoniutti, S.; Garcia-Fontan, S.; Carballo, R.; Padoan, F. *J. Chem. Soc., Dalton Trans.* **1998**, 2071.

(55) Luo, X.-L.; Kubas, G. J.; Burns, C. J.; Eckert, J. *Inorg. Chem.* **1994**, *33*, 5219.

non-hydrogen atoms appeared in subsequent difference maps. The *Cc* refinement, with all non-hydrogen atoms, failed to converge at this step at $R1 = 9\%$. Moreover, many atoms were nonpositive definite. A twin refinement in *Cc* corresponded to a perfect racemic mixture with $R1 = 9\%$ but did not converge. At this juncture, the refinement was converted to *C2/c* with the carbon and oxygen atoms of the carbonyl fixed at one-half occupancy. The refinement proceeded well and converged with no nonpositive definite atoms. The six-membered rings of the dppe ligands were refined as rigid bodies, with ring carbon-carbon distances fixed at 1.39 Å. No hydrogen atoms corresponding to a bound H_2 were found in a high angle difference map. All hydrogen atoms were fixed and refined in positions of ideal geometry. The C-H distances were fixed at 0.93 Å (ethyl) and 0.97 Å (phenyl). All hydrogen atoms were refined using the riding model in the HFIX facility in SHELX-93 and had their isotropic temperature factors fixed at 1.2 times the equivalent isotropic U of the atom they were bonded to. The final refinement included anisotropic thermal parameters on all non-hydrogen atoms.

Inelastic Neutron Scattering Studies. High-frequency data obtained at 15 K on the FDS instrument^{23b} at the Manuel Lujan Jr. Neutron Scattering Center of Los Alamos National Laboratory provided vibrational data, including transitions to the excited librational states (“torsions”) of the H_2 ligand. Low-frequency data could only be collected ($T = 5$ K) on the dppe compound using the cold neutron time-of-flight spectrometer IN5 at the Institut Laue-Langevin, Grenoble (France) and on the Mibemol spectrometer of the Laboratoire Léon Brillouin, Saclay (France). These data yield the tunnel splitting of the librational ground state of the coordinated H_2 .^{23c} Approximately 1–2 g samples, sealed under a partial H_2 atmosphere in quartz sample holders, were used for these experiments. The vibrational spectra were obtained with the aid of a spectral difference technique^{23d} that utilizes two samples, one with H_2 ligands and the other with D_2 , to subtract vibrations not associated with the H_2 ligand.

This work was supported by the Department of Energy, Office of Basic Energy Sciences, Chemical Sciences Division. The authors also thank Jean Huhmann-Vincent for organosilane reactions. This work has also benefitted from the use of facilities at the Manuel Lujan Jr. Neutron Scattering Center, a National User Facility funded as such by the Department of Energy, Office of Basic Energy Sciences.

Appendix. Derivation of equations for determining H-H and Mn-H distance by T_1 measurements. In all cases $R = 1/T_1$.

$$R_{HH} = \frac{3\gamma_H^4 (h/2\pi)^2}{10r_{HH}^6} \{ \tau_c/(1 + \tau_c^2\omega_H^2) + 4\tau_c/(1 + 4\tau_c^2\omega_H^2) \}$$

$$R_{HD} = \frac{2\gamma_H^2\gamma_D^2 (h/2\pi)^2}{15r_{HD}^6} S(S+1) \{ \tau_c/(1 + \tau_c^2\omega^2) + 3\tau_c/(1 + \tau_c^2\omega_H^2) + 6\tau_c/(1 + \tau_c^2\omega + 2) \}$$

$$\gamma_H = 2.675 \times 10^4 \text{ rads}^{-1} \text{ gauss}^{-1}$$

$$\gamma_D = 4.107 \times 10^3 \text{ rads}^{-1} \text{ gauss}^{-1}$$

$$\tau_c = 0.63/\omega_H \quad \omega_H = 2\pi(300 \times 10^6) = 1.88 \times 10^9 \text{ rad s}^{-1}$$

$$\tau_c = 3.34 \times 10^{-10} \text{ rad}^{-1} \text{ s}$$

$$S = 1$$

$$\omega_D = 2\pi(46.2 \times 10^6) = 2.90 \times 10^8 \text{ rad s}^{-1}$$

$$\omega_- = \omega_H - \omega_D = 2.17 \times 10^9 \text{ rad s}^{-1}$$

$$\omega_+ = \omega_H + \omega_D = 1.59 \times 10^9 \text{ rad s}^{-1}$$

$$3\gamma_H^4 (h/2\pi)^2 / 10 = 1.71 \times 10^{-37}$$

$$2\gamma_H^2\gamma_D^2 (h/2\pi)^2 / 15 = 1.79 \times 10^{-39}$$

$$\tau_c/(1 + \tau_c^2\omega_H^2) = 2.39 \times 10^{-10}$$

$$4\tau_c/(1 + 4\tau_c^2\omega_H^2) = 5.18 \times 10^{-10}$$

$$R_{HH} = (1.29 \times 10^{-46})/r_{HH}^6$$

$$\tau_c/(1 + \tau_c^2\omega_-^2) = 2.60 \times 10^{-10}$$

$$3\tau_c/(1 + \tau_c^2\omega_H^2) = 7.18 \times 10^{-10}$$

$$6\tau_c/(1 + \tau_c^2\omega_+^2) = 1.31 \times 10^{-9}$$

$$R_{HD} = (8.20 \times 10^{-48})/r_{HD}^6$$

$$R_{HMn} = \frac{2\gamma_H^2\gamma_{Mn}^2 (h/2\pi)^2}{15r_{HMn}^6} S(S+1) \{ \tau_c/(1 + \tau_c^2\omega_-^2) + 3\tau_c/(1 + \tau_c^2\omega_H^2) + 6\tau_c/(1 + \tau_c^2\omega_+^2) \}$$

$$\gamma_{Mn} = 6.598 \times 10^3 \text{ rads}^{-1} \text{ gauss}^{-1}$$

$$S = 5/2$$

$$\omega_{Mn} = 2\pi(74.1 \times 10^6) = 4.66 \times 10^8 \text{ rad s}^{-1}$$

$$\omega_- = \omega_H - \omega_{Mn} = 2.35 \times 10^9 \text{ rad s}^{-1}$$

$$\omega_+ = \omega_H + \omega_{Mn} = 1.41 \times 10^9 \text{ rad s}^{-1}$$

$$2\gamma_H^2\gamma_{Mn}^2 (h/2\pi)^2 / 15 = 4.61 \times 10^{-39}$$

$$\tau_c/(1 + \tau_c^2\omega_-^2) = 2.73 \times 10^{-10}$$

$$3\tau_c/(1 + \tau_c^2\omega_H^2) = 7.18 \times 10^{-10}$$

$$6\tau_c/(1 + \tau_c^2\omega_+^2) = 1.24 \times 10^{-9}$$

$$R_{HMn} = (9.01 \times 10^{-47})/r_{HMn}^6$$

Derivation of equation for Mn-H distance:

$$R_{HH(\text{obs})} = R_{HH} + R_{HMn} + R_{Hligand} \quad R_{Hligand} \approx 0$$

$$R_{HH(\text{obs})} = R_{HH} + R_{HMn}$$

$$R_{HH(\text{obs})} = (1.29 \times 10^{-46})/r_{HH}^6 + (9.01 \times 10^{-47})/r_{HMn}^6$$

$$r_{HH}^6 (1.21 \times 10^{-46}) / (R_{HH(\text{obs})} - R_{HD(\text{obs})})$$

$$R_{HH(\text{obs})} = (1.29 \times 10^{-46}) / (1.21 \times 10^{-46}) (R_{HH(\text{obs})} - R_{HD(\text{obs})}) + (9.01 \times 10^{-47})/r_{HMn}^6$$

$$R_{HH(\text{obs})} = 1.07 (R_{HH(\text{obs})} - R_{HD(\text{obs})}) + (9.01 \times 10^{-47})/r_{HMn}^6$$

$$R_{HH(\text{obs})} - 1.07(R_{HH(\text{obs})} - R_{HD(\text{obs})}) = (9.01 \times 10^{-47})/r_{HMn}^6$$

$$R_{HH(\text{obs})} - 1.07R_{HH(\text{obs})} + 1.07R_{HD(\text{obs})} = (9.01 \times 10^{-47})/r_{HMn}^6$$

$$1.07R_{HD(\text{obs})} - 0.07R_{HH(\text{obs})} = (9.01 \times 10^{-47})/r_{HMn}^6$$

R must be in s^{-1} and distance r is in cm. NMR constants were taken from ref 13b. τ_c is assumed to be the same in all equations, an approximation also made in ref 13b.

Supporting Information Available: X-ray data for complexes 1–3 (crystal information, atomic coordinates, bond lengths and angles, anisotropic displacement factors, hydrogen coordinates, packing diagrams, labeled ORTEPS). This material is available free of charge via the Internet at <http://pubs.acs.org>.